A DYNAMIC LIGHT SCATTERING INVESTIGATION INTO THE DYNAMICS OF NON IDEAL TERNARY POLYMER SOLUTIONS

A thesis presented in partial fulfillment of the requirements for the degree of Doctor of Philosophy in Physics at Massey University

William Nash

2004

Acknowledgements

Firstly I would like to thank my supervisor, Professor Neil Pinder for his infinite patience, continued encouragement and detailed criticism throughout the project.

Secondly thanks must go to my cosupervisor Dr. Yacine Hemar who made the solutions and provided a passionate outlook on the work.

Thanks also to my cosupervisor Harjinder Singh.

I would also like to thank my family for their unconditional love and support throughout my darkest moments.

Finally, thank you to all my friends, both old and new, who have been there for me even when I had nothing to give. Special thanks go to Doug for providing an oasis of calm and continued computing assistance during the project.

Abstract

Dynamic light scattering has been used to investigate three different non ideal ternary polymer systems. The three systems investigated were sodium caseinate and xanthan aqueous solutions, guar and dextran aqueous solutions and dextran and pullulan aqueous solutions. All solutions have been investigated at a temperature of 25°C.

Sodium caseinate and xanthan aqueous solutions with total polymer concentrations ranging from 0.01% w/w to 0.15% w/w and ratios of sodium caseinate of x = 1:3, 1:2, 2:1, and 3:1 have been investigated.

Guar and dextran aqueous solutions with total polymer concentrations ranging from 0.01% w/w to 0.06% w/w at a ratio of guar to dextran of 1:6 have been investigated.

Dextran and pullulan aqueous solutions with total polymer concentrations ranging from 1% w/w to 10% w/w with ratios of dextran to pullulan of 1:3, 1:1, and 3:1 have been investigated.

The solution concentrations have been chosen to fall in the semi-dilute range, while still being miscible.

Three different methods of analysis have been applied to resolve the field autocorrelations function into a sum of decaying exponentials; CONTIN, CONTIN multiq, and a Kohlrausch-Williams-Watts fit.

These resulting decay rates have been interpreted using the theoretical method outlined by Sun and Wang.

The CONTIN multiq method provided the best overall fit to the data. The Sun and Wang method has not provided results which are consistent with those reported elsewhere in the literature. Additional theoretical effort must be applied to interpret the results from dynamic light scattering on these novel non-ideal systems.

Contents

1

Introduction

The dynamics of ternary solutions has been an area of growing interest in many disciplines. The world around us is filled with examples of polymers, be they biological or synthetic in origin. Much of the production of polymer products involves the use of solvents of some kind, so whether the interest lies in producing novel blends of plastics or food with specific textures and tastes it is essential to know the properties of the constituent polymers or biopolymers in solution, how fast they move and the strength of the thermodynamic interactions between them.

Laser light scattering is seen as a good investigative tool to use on polymer solutions as it is a non invasive way of probing the density fluctuations in the solutions. Static light scattering measures the average intensity due to fluctuations in the density of the medium. Dynamic light scattering (DLS) gives a time dependent intensity autocorrelation function, which compares the intensity at time t_0 with the intensity at a later time t_1. With the advent of modern digital autocorrelators intensity autocorrelation functions can be found rapidly and provide a useful method of determining dynamical quantities in solution.

In the last two decades great effort has been expended to describe polymers in solution; this trend began with the investigation of polymers of one species in very dilute solutions. Dilute solutions are useful for determining parameters such as the size of the particles, the thermodynamic interaction between the polymers used and the rate of diffusion of the polymers in solution. Thus light scattering can be used to characterize polymers or biopolymers according to their properties in different solvents.[1]

If the aim is to synthesize polymers in solution and then extract them using some process the concentration of polymers will increase steadily until no solvent is left. In order to better control such processes it is useful to know how the thermodynamic properties of the solutions change over concentration and temperature. Light scattering work has been extended to the study of concentrated solutions of polymers.

The desire to understand the properties of blends of unlike polymers encouraged experimentalists and theorists alike to use the method of dynamic light scattering to study blends of two polymers (melts) or ternary solutions in the form of two polymers dissolved in a low molar mass solvent. As the solvent molecules are so much smaller than the polymers they scatter very little light, and consequently both melts and ternary solutions can be considered using the same formalism. Food and industrial applications often require high concentrations of polymer, and much work has been carried out on the study of ideal ternary polymer systems at concentrations above the overlap concentration (roughly the concentration at which the polymers would fill the whole volume) from both a theoretical[2-12] and an experimental[13-33] approach.

As the match between theory and experiment was promising the approach has been extended to ternary systems involving one ideal (synthetic) polymer, and one non ideal system[34].

This work was a natural extension of the body of work done on ideal and non ideal polymer systems. Its aim was to collect data on various ternary solutions and interpret the results in terms of the theory developed by Akcasu[2] and extended by Sun and Wang[11, 12] into a theory couched in experimental terms applicable to uncharged linear flexible homopolymers. The solutions chosen were xanthan/sodium caseinate, guar/dextran, and dextran/pullulan. Xanthan and sodium caseinate were chosen because they are of great interest to the food industry, altough they are least like the polymers described in the theory. Guar is also important to the food industry and is neutral and flexible in aqueous solution[35]. Dextran is important mainly in the medical sector as a blood volume expander and was chosen as it closely fits the requirements of the theory. However dextran is hyperbranched, with the branching becoming more pronounced as the molecular weight increases[36]. For this reason, low molecular weight samples of dextran were used. Pullulan was mainly chosen because it fits the requirements of the theory closely, the main deviation being that polysaccharides tend to have charged regions (as opposed to the neutral polymers normally investigated using this theory) or slight differences in the monomers along the length.

1.1 Thesis Structure

This thesis is structured in the following way:

Chapter 1. The introduction

Chapter 2. The theoretical models used to study multicomponent polymer systems are explored with a view to using dynamic light scattering as an experimental tool. This section describes the different approaches used to describe the density fluctuations in polymeric solutions. It details the developments in the theory from its early beginnings with applicability to a small set of polymers under certain fixed conditions, to a theory which may be applied to polymers with arbitrary properties. The theory as used in an experimental setting for binary solutions is given in section 2.2, while the corresponding theory for ternary solutions is summarized in section 2.3. Lastly, a section is presented on the thermodynamics; this is mainly to emphasize the connection between the Flory interaction parameter investigated by light scattering and the phase regime of the polymer mixtures.

Chapter 3. A brief overview of the nature of polysaccharides is presented, as these are the objects under investigation. A terse description follows of the biopolymers used: viz. guar, xanthan, sodium caseinate, dextran and pullulan.

Chapter 4. As the method used here was based on light scattering, a description of the essential theory underpinning the experimental method is provided to make clear the connection between the first principles given by Maxwell's equations and the density fluctuations from which the experimental parameters were extracted.

Chapter 5. A description of the experimental set up is presented.

Chapter 6. The results from the three different solutions are presented.

Chapter 7. The conclusions are presented, and future directions are discussed.

2

Theoretical models of Ternary Polymer Solutions

The study of polymer/polymer/solvent systems is of considerable importance in many areas. These include food science, medical science, and the cosmetics industry, not to mention the importance of plastics production. In order to facilitate the production of food with particular properties on an industrial scale, or to deliver drugs in a precise manner, it is essential to develop and test theories of polymer/polymer interactions and dynamics. Dynamic light scattering is an appealing tool to use on ternary systems, because it allows the study of complex systems from a non invasive point of view, and allows the determination of the motion of individual molecules and the interactions between unlike polymers. When using dynamic light scattering on ternary polymer solutions it is natural to use theories based on density fluctuations in solution. The theory presented was developed using operator projectors on the densities of the polymers, and has been developed from a theory which moves from microscopic entities to the measurable quantities available to an experimentalist. Over time the applicability of the theory has been widened by relaxing the constraints on the prameters used in the theory - from ternary solutions which differ only in molecular mass, to solutions with specific optical characteristics and finally to solutions with no constraints on them. The theory has been widely tested on ternary solutions of ideal polymers, and on some hybrid systems of polysaccharides and ideal polymers. This chapter seeks to inform the reader first of the framework the theory belongs to and the basic approach used to model multi component polymer systems, then to explain the relationship between the measured quantities and the microscopic properties of the solution, namely the translational self diffusion coefficient and the Flory-Huggins interaction parameter. The way in which these derived quantities relate to the bulk properties of the solution such, as the proximity to phase separation, is then explored.

2.1 General Formalism of Ternary Polymer Solutions

There are several different ways of formulating the problem of theoretically describing the dynamic structure factor. Theories of DLS from ternary polymer solutions can be found in many papers [2-12]. These theories are too numerous to be discussed in depth, and the more detailed microscopic theories are left out. Of these theories, perhaps the most widely used is that from Benmouna et al.[5], they provide as a starting point

$$S(q,t)=\sum_i\sum_j a_i\, a_j\, S_{ij}(q,t) \qquad 2.1.1$$

a_i are the increments of refractive indices for polymer i, and q is the scattering vector ($q = 4\pi n \sin(\theta)/\lambda$, where n is the refractive index of the solvent, and θ is the scattering angle). The total intermediate scattering function $S(q,t)$ is a sum of the contributions of scattered light from species i and j, $S_{ij}(q,t)$ is also a sum of different contributions, this time of light scattered due to the particles of species i, denoted $S_{ij}^{0}(q,t)$, and light scattered off the interactions between species i and j, denoted $Q_{ij}(q,t)$

$$S(q,t)=\delta_{ij}S_{ij}^{0}(q,t)+Q_{ij}(q,t) \qquad 2.1.2$$

Light is scattered by fluctuations in the dielectric constant, (since this is related to the density, often light is said to be scattered by density fluctuations) the fluctuations in density ($\delta\rho_i$) are given in Laplace space by

$$\delta\rho_i(q,s)=-\chi_{ii}^{0}(q,s)\left(\delta U_i(q,s)+\sum_j \nu_{ij}\delta\rho_j(q,s)\right) \qquad 2.1.3a$$

or

$$\delta\rho_i(q,s) = -\sum_j \chi_{ij}(q,s)\,\delta U_j(q,s) \qquad 2.1.3b$$

$\delta U_i(q,s)$ is an external excitation, $\chi^0_{ii}(q,s)$ is the bare response function and $\chi_{ij}(q, s)$ is the response function for the interacting system. v_{ij} are the excluded volume parameters for pairs of monomers of type i and j. Benmouna et al.[5] present equations for $\chi_{ij}(q, s)$ in terms of $\chi^0_{ii}(q,s)$ and v_{ij} and equations for $S_{ij}(q)$ in terms of $S^0_{ii}(q)$ and v_{ij}.

$$s_{11}(q) = \frac{s^0_{11}(q)\,(1+v_{22}\,s^0_{22}(q))}{(1+v_{11}\,s^0_{11}(q))(1+v_{22}\,s^0_{22}(q)) - v_{12}v_{21}s^0_{11}(q)\,s^0_{22}(q)} \qquad 2.1.4a$$

$$s_{12}(q)\frac{v_{12}\,s^0_{12}(q)\,s^0_{21}(q)}{(1+v_{11}\,s^0_{11}(q))(1+v_{22}\,s^0_{22}(q)) - v_{12}v_{21}s^0_{11}(q)\,s^0_{22}(q)} \qquad 2.1.4b$$

Another set of equations is needed to relate the response functions to the structure factors

$$kT\chi^0_{ii}(q,t) = -\partial_t S^0_{ii}(q,t) \qquad 2.1.5$$

and

$$s_{ij}(q) = kT\chi_{ij}(q,t) \qquad 2.1.6$$

This approach uses the random phase approximation (RPA)[37] to describe the total response functions in terms of the bare response function. Equations 2.1.1 -2.1.6 relate the structure factor to the density fluctuations. In order to find the time dependence of the dynamic structure matrix $S(q,t)$ (the matrix formed from with elements $S_{ij}(q,t)$) it is assumed that this matrix evolves over time following the simple exponential form

$$S(q,t) = \exp(-\Omega t) S(q) \qquad 2.1.7$$

This equation is used as a short term approximation, as it neglects the contribution of a memory term in the Langevin equation. Ω is defined as

$$\Omega(q) = -\lim_{t->0} \partial_t \left(S(q,t) \cdot S^{-1}(q) \right) \qquad 2.1.8$$

Equation 2.1.7 may be solved for $S(q, t)$ so that the terms $S_{ij}(q, t)$ appear as a sum of two exponentials. Generally, $S_{ij}(q, t)$ may be expressed as

$$S_{11}(q,t) = a_1 \exp(-\Gamma_1 t) + a_C \exp(-\Gamma_C t) \qquad 2.1.9$$

$$S_{21}(q,t) = b_1 \exp(-\Gamma_1 t) + b_C \exp(-\Gamma_C t) \qquad 2.1.10$$

where Γ_1 and Γ_C are the exponential decay rates (the eigenvalues of matrix Ω) given as

$$\Gamma_1 = \Omega_{av} - \sqrt{\Omega_{av}^{\ 2} - \Delta(\Omega)} \qquad 2.1.11$$

$$\Gamma_C = \Omega_{av} + \sqrt{\Omega_{av}^{\ 2} - \Delta(\Omega)} \qquad 2.1.12$$

Ω_{av} and $\Delta(\Omega)$ are equal to half the trace and the determinant of the 2 x 2 matrix Ω respectively, and the amplitudes a_1, a_C, b_1, b_C,given by

$$a_1 = \frac{(\Gamma_1 - \Omega_{22}) S_{11}(q) + \Omega_{12} S_{21}(q)}{\Gamma_1 - \Gamma_C} \qquad 2.1.13$$

$$a_C = \frac{(\Gamma_C - \Omega_{22}) S_{11}(q) + \Omega_{12} S_{21}(q)}{\Gamma_C - \Gamma_1} \qquad 2.1.14$$

$$b_I = \frac{(\Gamma_I - \Omega_{11})\, S_{21}(q) + \Omega_{21}\, S_{11}(q)}{\Gamma_I - \Gamma_C} \qquad 2.1.15$$

$$b_C = \frac{(\Gamma_C - \Omega_{11})\, S_{21}(q) + \Omega_{21}\, S_{11}(q)}{\Gamma_C - \Gamma_I} \qquad 2.1.16$$

S_{22}(q,t) and S_{12}(q,t) are found by interchanging indices in equations 2.1.9-2.1.10. The quantities appearing in S_{ij}(q) can be related back to the bare scattering matrices $s_{ii}^0(q)$ by equations 45a and b of Wang[12]

$$s_{ii}^0(q) = x_i \phi N_i P_i(q) \qquad 2.1.17$$

where x_i is the fraction of polymer i present, ϕ is the total segmental concentration, N_i is the polymerization of polymer i and $P_i(q)$ is the wave-vector dependent form factor. x_i, ϕ, and N_i are all experimental variables and combined with $P_i(q)$ determine $S_{ii}^0(q)$, that with v_{ij} determine the values of $S_{ii}(q)$ that appear in eqs. 2.1.4a and 2.1.4b. The remaining variables in eq 2.1.13 are the matrix elements Ω_{ij}. Using eqs. 2.1.5, 2.1.6, and 2.1.8, and introducing the mobility matrix $M(q)$ which relates the forces on particles to velocities of particles[38]. The elements of $M(q)$ are defined as

$$M_{ij}(q) = q^{-2} \lim_{s->\infty} s\chi_{ij}(q,s) \qquad 2.1.18$$

where $\chi_{ij}(q,s)$ is the Laplace transform of $\chi_{ij}(q,t)$, it is shown in ref. 5 that

$$\Omega = q^2 kTM(q) \cdot S^{-1}(q) \qquad 2.1.19$$

A simple form of $M_{ij}(q)$ is obtained when using a Rouse model of dynamics, in which there is no hydrodynamic interaction between different blobs (an interpolation formula for the size of these blobs is expressed in ref. 9), and with no Zimm type of hydrodynamic

interaction[38]. Such approximations are only used in the semi dilute and concentrated regimes, and when employed the matrix elements $M_{ij}(q)$ are determined by

$$M_{ij}(q) = \frac{\delta_{ij}\,\phi}{\xi} \qquad 2.1.20$$

δ_{ij} is the Kronecker delta function. $\mathbf{M}(q)$ is therefore a diagonal matrix with entries proportional to segment density ϕ_i and inversely proportional to a friction coefficient ξ. Alternate forms of $\mathbf{M}(q)$ that include off diagonal terms (which are important for dilute solutions) are found in refs. 9, 21,39, and 40. Benmouna et al.[5] use the Rouse value of $\mathbf{M}(q)$ to describe Γ_I and Γ_C in terms of χ, υ, ϕ, N, $P(q)$, and x.

$$\Gamma_I = \Gamma_0(q)(1 - 2\phi\chi x(1-x)NP(q)) \qquad 2.1.21$$

$$\Gamma_C = \Gamma_0(q)(1 + \nu\phi NP(q)) \qquad 2.1.22$$

This is done under the assumption of identical polymerization's ($N_1 = N_2 = N$), the same interaction parameter with the solvent ($\nu_{11} = \nu_{11} = \nu$) , and with $\nu_{12} = \nu + \chi$. The contrast factor a_2 is set to zero so that only the component $S_{11}(q, t)$ of the total scattering matrix is visible (This is known as the isorefractive condition). The q^2 dependence of $\Gamma_0(q)$ is written as

$$\Gamma_0(q) = q^2 \frac{kT}{\xi NP(q)} \qquad 2.1.23$$

Equations 2.1.21 & 2.1.22 are valid only for systems in which the polymers are not incompatible and the solvent is good for both the polymers i.e. under the condition that $\chi/\nu << 1$. Equation 2.1.21 can be expressed simply as

$$\Gamma_I = \Gamma_0(q)\left(1-\frac{\chi}{\chi_c}\right) \qquad 2.1.24$$

with

$$\chi_c = \frac{1}{2\phi\, x(1-x)NP(q)} \qquad 2.1.25$$

To see why Γ_I is written in such a suggestive form it is useful to define the spinodal curve at this point. In the case of light scattering the spinodal equation is defined as the condition which causes $S_{11}(q, t)$ to tend toward infinity.
This is the condition that

$$\left(1 + \nu_{11}\, s_{11}^0(q)\right)\left(1 + \nu_{22}\, s_{22}^0(q)\right) - \nu_{12}\nu_{21} s_{11}^0(q)\, s_{22}^0(q) = 0 \qquad 2.1.26$$

which, under the simplifications used in eqs. 36 & 37 of ref. 5, is easily solved for

$$\chi_c = \frac{1+N\nu\phi P}{2(NP\phi)^2(x-1)x\nu} \qquad 2.1.27$$

which in the limit of high concentration ($\nu\phi N >> 1$) reduces to

$$\chi_c = \frac{1}{2(NP\phi)(x-1)x} \qquad 2.1.28$$

equation 2.1.28 and 2.1.25 are the same, and it is seen that in the high concentration regime $\Gamma_I = 0$ when $\chi = \chi_c$. Physically, the interdiffusion coefficient must change from being positive to negative in order for instabilities to grow and phase separation to occur. This represents individual components climbing up their concentration gradients, and, thus creating regions of space in which one species or the other are present in much greater quantities than its opposite. A good description of this process is found in "An Introduction

to Dynamics of Colloids"[41]. The theory presented above has been tested experimentally by Borsali et al.[14] who used a ternary solution of polystyrene(PS)/Polymethylmethacrylate(PMMA)/toluene, solutions of PMMA and toluene are isorefractive and so the only light scattered in such systems is due to fluctuations in the PS density. This enables one to see the effect the PMMA/toluene matrix (solution) on PS, and this condition (setting $a_2 = 0$ in equation 2.1.1) makes the calculations much simpler. The experiment was divided into two parts, one part detailing the solutions of PS in toluene in the dilute and semi-dilute regimes and the other detailing the concentrated ternary solutions. In the first part they detected only one mode (a fast mode) they plotted the determined D (where $D = q^2 \Gamma$) by plotting Γ against q^2 (see fig. 4 of ref. 42) and plotted log$D$ vs log$C$ to find a power law dependence of D, namely D = 3.64 x 10^{-6} $c^{0.51}$cm^2/s. In the second part they found that the measured autocorrelation signal depended on the sampling window times used (17μs and 450μs in this case). At slow sampling times the correlation signal contained information about the interdiffusion coefficient, while at fast times it contained information about the collective diffusion coefficient. They concluded that, if only semi-qualitatively, there was good agreement between the theory of Benmouma et al.[5] and the experiments.

The relaxation coefficients Γ_I & Γ_C (as defined in eqs. 2.1.11 & 2.1.12) are often interpreted as the interdiffusion coefficient and the cooperative diffusion coefficient respectively this is how they are used in refs. 5 & 14 in fact they are the eigenvalues of Ω. This is shown in Wang's paper outlining his theory of light scattering from ternary polymer solutions[12] and in more detail by Akcasu et al.[4] (see below). Wang's starting point is to define total polymer concentration (δc) and composition variables (δx) (instead of the usual concentration of polymer 1 and 2) as

$$\delta_C = \delta(\rho_1 + \rho_2) \qquad 2.1.29$$

$$\delta x = \frac{(x_1 \delta\rho_1 - x_2 \delta\rho_2)}{\rho_T} \qquad 2.1.30$$

by transforming between the two variables δc and δx and the variables $\delta\rho_1$ and $\delta\rho_2$, the time correlation function denoted $G(q,t)$ by Wang[12] may be written as

$$G(q,t)=(x_1\varepsilon_1+x_2\varepsilon_2)^2 S_{CC}+\rho_T(x_1\varepsilon_1+x_2\varepsilon_2)(\varepsilon_1-\varepsilon_2)(S_{CX}+S_{XC})+\rho_T(\varepsilon_1-\varepsilon_2)^2 \qquad 2.1.31$$

In this equation, S_{CC}, S_{XX}, S_{CX}, S_{XC} are the autocorrelation and cross correlation functions for δc and δx respectively (the q and t dependence has been suppressed for simplicity). Eqs. 53a-d in ref. 12 give S_{CC}, S_{XX}, S_{CX}, S_{XC} explicitly in terms of S_{11}, S_{22}, S_{12}, S_{21}, x_1, x_2, and ρ_T it is seen from these four equations that S_{CX} and S_{XC} are not generally zero and, thus, δc and δx are coupled unless the two polymer species differ essentially only in labelling, which would not be the case if they (δc and δx) were eigenmodes associated with rates Γ_I and Γ_C (as defined in eqs. 2.1.11 & 2.1.12). From equation 2.1.31 a second special optical condition is observed. If

$$x_1\varepsilon_1+x_2\varepsilon_2=0 \qquad 2.1.32$$

then equation 2.1.31 becomes

$$G(q,t)=\rho_T(\varepsilon_1-\varepsilon_2)^2 S_{XX} \qquad 2.1.33$$

In this case, the total autocorrelation function depends only on the optical factors ε_1 and ε_2 (equivalent to a_1 and a_2 in eqn 2.1.1), the total equilibrium polymer concentration ρ_T and on S_{XX}, the composition autocorrelation concentration. Equation 2.1.32 is known as the zero average contrast condition and is employed to view composition fluctuations these fluctuations and the way they decay are indicative of the compatibility of the two polymer species.

The theory presented in Wang[12] is of much the same form as Benmouma et al.[5], except that Wang's theory is applicable to a wider range of polymer systems, as it relaxes the assumptions of equal friction coefficients and solvent affinity. Wang's work is grounded in

the formalism that is presented in detail by Akcasu[2]. This formalism is summarized by Akcasu et al.[4] in a work designed to show that the identification of Γ_I and Γ_C (the eigenvalues of Ω) as the interdiffusion and cooperative diffusion modes is incorrect. This is done by first finding the eigenmodes of the system (a linear combination of the two polymer concentrations) , and then showing that neither of the two linear combinations $\rho_+ = \rho_a + \rho_b$ or $\rho_- = \rho_a/N_1 - \rho_b/N_2$ (which are the concentration and composition variables) are equal to one of the eigenmodes. Akcasu et al.[4] go further in the exploration of diffusion coefficients and a summary of their work is given here.

By matching the initial slope of a desired single exponential form of the composition autocorrelation function with that of the double exponential that theory predicts, the interdiffusion coefficient is defined as

$$D_{in} = kT \frac{\frac{\mu_{aa}}{N_a^2} - 2\frac{\mu_{ab}}{N_a N_b} + \frac{\mu_{bb}}{N_b^2}}{\frac{s_{aa}}{N_a^2} - 2\frac{s_{ab}}{N_a N_b} + \frac{s_{bb}}{N_b^2}} \qquad 2.1.34$$

where N_a and N_b are the numbers of polymer type a and b respectively and μ_{aa}, μ_{ab} and μ_{bb} are elements of the mobility matrix (as defined with slightly different notation in eqn. 2.1.19). By a similar process, D_{coop} is found

$$D_{coop} = kT \frac{\mu_{aa} + \mu_{bb} + 2\mu_{ab}}{s_{aa} + s_{bb} + 2s_{ab}} \qquad 2.1.35$$

They show that it is possible to express D_{in} as the product of a kinetic factor (Λ_{in}) and a thermodynamic factor ($1/S_{00}$). The kinetic factor is given by the Green-Kubo formula

$$\Lambda_{in} = \int_0^\infty \langle J(t)J(0)\rangle dt \qquad 2.1.36a$$

where J is the long term limit of the longitudinal interdiffusion current

$$J(t)=\frac{1}{N_a}\sum_{i=1}^{N_a}v_i^a(t)-\frac{1}{N_b}\sum_{j=1}^{N_b}v_j^b(t) \qquad 2.1.36b$$

If the vector separation between the centre of mass of components is given as

$$\mathbf{R}_{in}(t)=\frac{1}{N_a}\sum_{i=1}^{N_a}\mathbf{R}_i^a(t)-\frac{1}{N_b}\sum_{j=1}^{N_b}\mathbf{R}_j^b(t) \qquad 2.1.36c$$

then $J(t)$ can be written $J(t) = (d/dt)Z_{in}$, where Z_{in} is the z-component of $\mathbf{R}_{in}$. With these definitions in place there is an alternative, and perhaps more physical, definition for Λ_{in}

$$\Lambda_{in} = \lim_{t->0}\frac{1}{6t}\left\langle\left|\mathbf{R}_{in}(t)-\mathbf{R}_{in}(0)\right|^2\right\rangle \qquad 2.1.36d$$

Equations 2.1.36a-d relate the kinetic factor to the number of monomers of type A or B, and to the position and velocity coordinates of the individual monomers that are in solution. Such an approach allows one to use microscopic theories of particle motion to calculate the kinetic factor that appears in the approximation for the interdiffusion coefficient. Chapter 6 of ref. 41 contains a sound introduction to the problem of using microscopic theories of Brownian particles to calculate self and collective diffusion coefficients in binary solutions of particles in various limits of time and wave-vector values.

It is important to realize that Akcasu et al.[4] include a memory term in their equations this term occurs in the definition of **D** (the diffusivity matrix)

$$D=\lim_{q->0}\frac{1}{q^2}\left(\Omega(q)-\int_0^\infty du\phi(q,u)\right) \qquad 2.1.37$$

The integral term in eqn 2.1.47 is the memory term. ϕ is the autocorrelation function of the random force appearing in the generalized Langevin equation. Ω is the first cumulant matrix and in order to recover the short term behaviour of D the elements μ_{ab} must be replaced by m_{ab}. This is largely a matter of relabelling at present, as neither μ_{ab} or m_{ab} are defined, but it is of note, as Benmouna et al.[5] use a short time approximation. Ackasu[2] includes a memory term. Akcasu et al.[4] go through a number of examples of polymer systems to illustrate their theory.

The main purpose of Akcasu et al.'s[4] work is to compare D_{coop} and D_{in} with Γ_C and Γ_I (λ_- and λ_+ in ref. 12). They come to the conclusion that for D_{coop} and D_{in} to coincide with Γ_C and Γ_I the two different polymer chains A and B must differ from each other only by their labelling.

This paper uses a framework which allows a macroscopic result using microscopic input via the use of equation 7[4]

$$\rho(q,t) = -L\rho(q) \qquad 2.1.38$$

with $\rho = (\rho_a , \rho_b)$, L is an operator which can contain microscopic information about the polymer system. Ref. 41 gives a good physical description of the diffusion of Browning particles (and rods) in solution though it does not deal with multi-component systems, and while of interest on a theoretical and intuitive note, it is not a particularly useful guide to experimental work.

The subject of optical properties is explored experimentally in Geibel el al.[23] In this paper they report the results of DLS experiments on the PDMS/PMMA/Solvent system with toluene (isorefractive with PMMA) and Chloroform (chosen because it satisfies eqn. 2.1.32 at equal composition of PDMS and PMMA) the experiments were performed on systems at five times the overlap concentration (C =5C*, C* = $3M_W/(4\pi R_g^3)$) the concentration at which the polymers, if treated as spheres, would completely fill the solution volume by themselves. For PMMA/PDMS/toluene only the PDMS was seen for that system they kept the total polymer concentration constant and varied the composition (the ratio of PMMA to total polymer concentration). Two different diffusion coefficients were found in that case, one which varied as (1-x) x (D_I) and one which was independent

of composition (D_C). Fig. 1 of ref 23 shows that these two coefficients were found in all three polymer/solvent mixtures (toluene chloroform THF) and had the same form (if different exact values), comparing well with the form of Γ_1 and Γ_C in eqs. 2.1.21 and 2.1.22 respectively (Γ_1 and Γ_C equal q^2D_1 and q^2D_C respectively). Geibel et al.[23] used the algorithm devised by Provencher called CONTIN, which is extensively used to fit peaks to DLS data. The experiments on PDMS/PMMA/Chloroform showed that from $x = 0.4 \rightarrow x = 0.6$ (i.e. around the symmetric concentration point) only one mode was detected, while outside this range two were detected this was because the amplitude of this mode was close to zero near x = 0.5. Their data provide values of $(\nu\phi N)_{chlo} = 11.24$,$(\chi\phi N)_{chlo} = 1.14$ $(\nu\phi N)_{tol} = 7.21$, $(\chi\phi N)_{tol} = 1.32$, $(\nu\phi N)_{THF} = 7.85$, $(\chi\phi N)_{THF} = 1.50$ and $D_S = 5.4 \times 10^{-8}$ cm^2 s^{-2}. Dynamic light scattering experiments using the theories above (or slight variations of them) have been carried out by workers in the field[15,20,24,26,32,33] - of these Pinder[26] and Sun and Wang[32] are the most relevant to this work. Pinder[26] used pulsed field gradient nuclear magnetic resonance to obtain self diffusion coefficients of the polymers, and used this additional information to determine the polymer-polymer interaction parameters. Sun and Wang[32] used the relative amplitudes of the different decay rates as additional information to determine the self diffusion coefficients and the polymer-polymer interaction parameters.

The theories outlined above are mean field theories in that the potential energy of interactions between monomers is a mean (constant) value. These theories rely on the polymer solution being far from the spinodal curve (far from phase separation).
Benmouna et al.[39] explore the problem of critical fluctuations by using the zero average contrast condition and bringing the system from a stable state to a critical state or to a two phase state. This is done by lowering the temperature (which by eqn 2.4.8 increases χ and makes the system less stable) or by evaporation of solvent (which decreases the favourable entropy of mixing term). This paper outlines the essential results of the theory of ref. 5 and provides useful formulae relating the excluded volume parameters to the solvent volume fraction and the Flory-Huggins interaction parameters

$$\theta_{11} = \frac{1}{\phi_s} - 2\chi_{1s} \qquad 2.1.39a$$

$$\theta_{22} = \frac{1}{\phi_s} - 2\chi_{2s} \qquad 2.1.39b$$

$$\theta_{12} = \frac{\theta_{11} + \theta_{22}}{2} + \chi = \frac{1}{\phi_s} - \chi_{1s} - \chi_{2s} + \chi \qquad 2.1.39c$$

(in ref. 39 the excluded volume parameters are labelled as θ instead of v) and gives explicit equations for χ_C in terms of the interaction parameters, solvent volume fraction, polymerization and polymer species concentration. This critical value of χ is found as before by setting the denominator in eqs. 2.1.4a and 2.1.4b equal to zero. Near the critical point, or near phase separation, the correlation length in the solution increases. For extremely dilute solutions the correlation length is roughly equal to the radius of gyration of a polymer molecule, this represents the fact that within a polymer the monomers are all moving as one (when a sphere translates the points in or on it move together). For melts (the limit of high concentration) the correlation length is roughly the monomer size. An interpolation formula for this change in correlation length is given in ref. 9. When the correlation length is as large or larger than the wavelength being probed, the form factor of the polymer becomes important. The form factor is a function of the particle size. Benmouna et al.[39] use a crossover model for a polymer size. This models the size of particles by first defining a "blob" size (the number of monomers in a blob, N_0) and then saying if a string of monomers of length n is less than N_0 then the end to end length of this string is $R_n^2 = n^{2\nu} a^2$ and if n is greater than N_0 then $R_n^2 = (n/N_0)\xi_0^2$, where a is the statistical length of a monomer, ξ_0 is the blob or correlation length given by $\xi_0 = N_0^{2\nu} a^2$, and ξ_0 and N_0 scale with $\phi^{-3/4}$ and $\phi^{-5/4}$. With these results and the form factor given by the Debye formula

$$P(q) = \frac{2}{\left(q^2 R_g^{\,2}\right)^2}\left(e^{-q^2 R_g^{\,2}} + q^2 R_g^{\,2} - 1\right) \qquad 2.1.40$$

Benmouna et al.[39] use renormalization techniques to show

$$NP(q) = 1 + \frac{N_0}{v a_1^{\frac{1}{2v}}}\left\{F\left(\frac{1}{2v}, a_1\right) - \frac{Z}{a_1^{\frac{1}{2v}}}F\left(\frac{1}{v}, a_1\right)\right\} + \frac{2N}{a_2}\left\{\left((1-z)e^{-za_2} + \frac{1}{a_2}\left(e^{-a_2} - e^{-za_2}\right)\right)\right\} \qquad 2.1.41a$$

where F is defined as

$$F(\mu, a_1) = \gamma(\mu, a_1) - \gamma\left(\mu, \frac{a_1}{N_0^{\,2}}\right) \qquad 2.1.41b$$

γ is given by

$$\gamma(\mu, a_1) = \int_0^{a_1} dx\, x^{\mu-1} e^{-x} \qquad 2.1.41c$$

and a_1, a_2 and z are given by

$$a_1 = q^2\, \xi_0 / 6,\ a_2 = a_1 / z,\ z = N_0 / N \qquad 2.1.41d$$

The calculations involved in deriving eqn. 2.1.41a presume $\xi_0 < R_g$. Approximating equation 2.1.40 by

$$P(q) = \frac{1}{1 + \frac{1}{2} q^2 R_g^{\,2}} \qquad 2.1.42$$

and using this in the equation for S_T

$$S_T(q) = \frac{\phi NP(q)}{1 + (\theta + \chi/2)\phi NP(q)} \qquad 2.1.43$$

one finds

$$\frac{S_T(q)}{S_T(0)} = \frac{\xi_0^{-2}}{q^2 + \xi_0^{-2}} \qquad 2.1.44$$

These equations relate the light scattering component S_T to the correlation length of the concentration fluctuations. In a similar way S_I is related to composition fluctuations ξ

$$\frac{S_I(q)}{S_I(0)} = \frac{\xi^{-2}}{q^2 + \xi^{-2}} \qquad 2.1.45a$$

with

$$\frac{S_I(0)}{4\phi N} = \frac{\chi_C}{\chi_C - \chi} \qquad 2.1.45b$$

and

$$\xi = \frac{R_g}{2^{1/2}}\left(\frac{\chi_C}{\chi_C - \chi}\right)^{1/2} \qquad 2.1.45c$$

where

$$\chi_C = \frac{2}{\phi N} \qquad 2.1.45d$$

next a form of χ of the type in eqn. 2.4.8 (see section 4 below) is assumed and the scattering matrix due to composition fluctuations may be written in the form

$$\frac{S_I(0)}{4\phi N} = \frac{T_C \chi_C}{\chi_a}\left(\frac{T - T_C}{T}\right)^{-1} \qquad 2.1.46a$$

with

$$\xi = R_g\left(\frac{T_C \chi_C}{2\chi_a}\right)^{1/2}\left(\frac{T - T_C}{T}\right)^{-1/2} \qquad 2.1.46b$$

These equations are written in a form recognizable as variables near the critical point T_I. The subject of spinodal decomposition in polymer solutions, or the growth of fluctuations near this point is the subject of some studies[6, 27, 42, 43] - these are not looked at in depth here, and are included only to show that work on non equilibrium (perturbed) polymer systems is continuing using light scattering studies. Akcasu[42], in a theoretical paper, derives the total scattering intensity as a function of time in terms of initial intensity and the equilibrium intensity. The aim of ref. 42 is to derive the Cahn-Hillard-Cook theory from a microscopic perspective; this is achieved quite generally using a starting point credited to Mori (see ref. 42). Foley et al[6], also in a theoretical paper, predict three modes for quenched solutions - two which decay rapidly and one which increases. Lal et al.[43], in an experimental work, study the time evolution of the structure factor $S(k,t)$ at various times t after quenching PS-CH solutions to a temperature below the spinodal temperature. This study shows the growth of structure at a particular wave vector k_M, associated with a characteristic length of phase separated domains. Sasaki et al.[27] perform their spinodal decomposition study on ternary mixtures PS/Polybutadiene/toluene.

The area of ternary polymer solutions has been actively explored recently, this chapter is intended to briefly illustrate the theories and methods involved in measuring the Flory-Huggins interaction parameters and how they relate to the compatibility of the polymers.

2.2 The Dynamics of Binary Polymer Solutions

Dynamic light scattering measures the correlations in the light intensity scattered from the sample. The measured signal is the intensity autocorrelation function $G^{(2)}$. This quantity is transformed into the first order field autocorrelation function using the well used Seigert relationship. The field autocorrelation function $G^{(1)}$ is interpreted as being a sum of decaying exponentials; each decay rate is then related to the dynamics of the solution being probed. From the decay rates so determined the thermodynamic and hydrodynamic properties of the molecules in solution can be assessed

$$G^{(1)} = A\exp(-\Gamma t) \qquad 2.2.1$$

The decay rate is a function of both the scattering vector, $q = (4\pi n/\lambda)\sin^2(\theta/2)$, and concentration ($c$) binary polymer solutions can be characterized by the change in decay rates with respect to these two variables. The apparent diffusion coefficient is related to the measured decay rate by

$$\Gamma = q^2 D_{app}(q,c) \qquad 2.2.2$$

The mutual diffusion coefficient $D(c)$ can be determined from this equation by taking the limit of Γ / q^2 as q tends to zero

$$D(c) = D_{z,0}(1 + k_D c) \qquad 2.2.3$$

From this, $D_{z,0}$ and k_D can be extracted. The diffusion coefficient at zero concentration

$$D_{z,0} = \frac{kT}{f(0)} = \frac{kT}{6\pi n R_h} \qquad 2.2.4$$

gives the frictional coefficient $f(0)$ at infinite dilution, or the hydrodynamic radius R_h. The second hydrodynamic virial coefficient k_D is related to the second virial coefficient A_2 and the friction coefficient k_f by

$$k_D + k_f = 2A_2M_W - \nu \qquad 2.2.5$$

where M_W is the molecular mass of the polymer and ν is the partial specific volume of the polymer. There are various frameworks which associate the values so determined with the nature of the polymer, be it branched or linear, rod like or spherical and so on.
At higher concentrations the mutual diffusion coefficient is described by

$$D(c) = \frac{kT}{f(c)} \frac{M_W}{RT} \frac{d\Pi}{dc} \qquad 2.2.6$$

where $f(c)$ is the concentration dependent friction coefficient of individual chains, M_W the molecular weight, and Π the osmotic pressure. Ioan, Aberle and Burchard[44] provide a method for using eqn 2.2.6 in conjunction with static light scattering observations to determine the friction coefficient at higher concentrations. Unfortunately such measurements are not available to us, so the equations for low concentrations have been used instead.

Wang[45] provides a theoretical model for binary polymer solutions in the semidilute regime by considering the coupling between viscoelastic effects and concentration fluctuations.

2.3 The Dynamics of Ternary Polymer Solutions

Sun and Wang[31] succinctly describe the theory used here, while the general theory of light scattering from multicomponent polymer solutions is given by Akcasu[2]. The basic equations are represented here. The Intensity autocorrelation function measured by DLS is given by

$$S(q,t)=\sum_i\sum_j a_i\, a_j\, S_{ij}(q,t) \qquad 2.3.1$$

a_1 and a_2 are the refractive index increments of polymer 1 and 2. The equations regarding the diffusivity matrix are given in a form which facilitates experimental work. These values along with the relative amplitude are experimentally determined quantities. The elements of the **D** are related to other experimental parameters via eqs. 2.3.3-2.3.6

$$I(q,t)=A_{-}e^{-q^2D_{-}t}+A_{+}e^{-q^2D_{+}t} \qquad 2.3.2$$

$$D_{11}=\frac{D_{S1}}{P_1}\left(1+2xA_{2,11}M_{W1}c_TP_1\right) \qquad 2.3.3$$

$$D_{22}=\frac{D_{S2}}{P_2}\left(1+2(1-x)A_{2,22}M_{W2}c_TP_2\right) \qquad 2.3.4$$

$$D_{12}=D_{S1}xc_T2A_{2,12}M_{W1}\frac{m_2}{m_1} \qquad 2.3.5$$

$$D_{21}=D_{S2}(1-x)c_T2A_{2,12}M_{W2}\frac{m_1}{m_2} \qquad 2.3.6$$

It is through these four equations that the unknown elements D_{s1}, D_{s2} and $A_{2,12}$ are introduced. These quantities represent the self-diffusion coefficients of the two polymer species and $A_{2,12}$ is the cross second virial coefficient between polymers 1 and 2. The parameters in eqs. 2.3.3-2.3.6 are the composition (x), the total polymer concentration in g/mL (C_T), the molecular weight of polymer i in g/mol (M_{Wi}), the second virial coefficient of polymer i ($A_{2,\,ii}$), the relative monomer molecular masses (m_1/m_2) and the form factors of polymer i (P_1 and P_2). The Debye formula[30] has been used to determine the form factors when $qR_g > 1$.

The elements of **D** are related to the experimentally determined eigenvalues and the relative amplitudes by eqs. 2.3.7 –9

$$D_+ + D_- = D_{11} + D_{22} \qquad 2.3.7$$

$$D_+ D_- = D_{11} D_{22}(1 - XY) \qquad 2.3.8$$

$$\frac{A_-}{A_- + A_+} = \frac{D_+}{D_- + D_+}\left(1 - D_- \frac{a_2{}^2 X/D_{11} + a_1{}^2 X/D_{22}}{a_1{}^2 Y - 2a_1 a_2 XY + a_2{}^2 X}\right) \qquad 2.3.9$$

X and Y are

$$X = \frac{D_{21}}{D_{22}} \qquad 2.3.10$$

$$Y = \frac{D_{12}}{D_{11}} \qquad 2.3.11$$

Using eqns. 2.3.3-2.3.6, the eqns. 2.3.7-2.3.9 can be solved for D_{s1}, D_{s2} and $A_{2,\,12}$. $A_{2,\,12}$ is related to the Flory-Huggins polymer-polymer interaction parameter by

$$\chi_F = V_S\left(\frac{2A_{2,12}}{v_1 v_1} - \frac{A_{2,11}}{v_1^{\,2}} - \frac{A_{2,22}}{v_2^{\,2}}\right) \qquad 2.3.12$$

V_s is the molar volume of the solvent, and v is the specific volume of polymer i.
This theory relaxes the assumptions previously used and allows one to apply the theory to ternary solutions with arbitrary solution properties.

2.4 Thermodynamic Effects in Ternary Polymer Solutions

By far the most common way to approach the problem of determining the interactions between polymers in solution is to first set up a Gibbs free energy of mixing equation. There are a number of slightly different equations used for this, see for instance Hsu & Prausnitz[46], Koningsveld et al.[47, 48], Solc[49], and almost any book relevant to polymer solutions[50-52]. All these forms of Gibbs free energy of mixing contain the classical entropy of mixing terms and a second term which is quadratic in a combination of polymer1, polymer2 and solvent fraction. This second term has a coefficient which is related to the energy interaction parameters between polymer1, polymer2 and the solvent.

$$\frac{\Delta G^m}{RT} = n_0 \ln\phi_0 + n_1 \ln\phi_1 + n_2 \ln\phi_2 + n_0 r_0\left(\phi_1 g_1 + \phi_2 g_2\right) + n_1 r_1 \phi_2 g_x \qquad 2.4.1$$

$$\frac{\Delta G^m}{RT} = n_0 \ln\phi_0 + n_1 \ln\phi_1 + n_2 \ln\phi_2 + g n_1 \phi_2 \qquad 2.4.2$$

$$\frac{\Delta G^m}{RT} = n_1 \ln\phi_1 + n_2 \ln\phi_2 + n_s \ln\phi_s + \left(\chi_{12}\phi_1\phi_2 + \chi_{13}\phi_1\phi_3 + \chi_{2s}\phi_2\phi_s\right)\left(m_1 n_1 + m_2 n_2 + m_s n_s\right) \qquad 2.4.3$$

where ϕ_1, ϕ_2, ϕ_0 or ϕ_s are the volume fractions of polymer1, polymer2 and solvent respectively, n_1, n_2, n_0 or n_s are the numbers of moles of polymer1, polymer2 and solvent respectively. m_i is the ratio of the molar volume to that of a reference component. These three equations come from refs. 49, 48 and 46 respectively, the first three terms on the right hand side of eqs. 2.4.1-2.4.3 are the combinatorial (entropic) terms (ϕ_s is identical to ϕ_0) and the others are the energy of interaction terms.

Equation 2.4.2 is the simplest of these with an energy of mixing term $g\, n_1 \varphi_2$. Paul and Barlow[53] (talking about blends) provide examples in which measured heats of mixing are clearly non parabolic, which means that g (or χ) cannot be a simple constant but must at the very least depend on composition. They also point out that for high molecular weight polymers, the entropic terms are small and nearly zero for the high molecular weights of many commercially important polymers. Paul and Barlow[53] are talking about polymer blends, but from equations 2.4.1-2.4.3 it is clear that of the three entropic parts, the part due to the solvent is of most importance. That the polymer entropy terms tend to zero with molecular weight is clearer from equation 2.4.4[54]

$$\frac{\Delta G}{RT} = \frac{\phi_A \ln \phi_A}{N_A} + \frac{\phi_B \ln \phi_B}{N_B} + \phi_v \ln \phi_v + \chi \phi_A \phi_B \qquad 2.4.4$$

with N_A and N_B being the degree of polymerization of polymers A and B respectively, and $\phi_V = \phi_0$.

All the detail regarding polymer compatibility is contained in the parameters attached to the terms quadratic in ϕ these parameters are given different labels and refer to slightly different things in the different equations. Equations 2.4.1 and 2.4.2 have three different parameters, one for each of the possible combinations of ϕ_0 , ϕ_1 and ϕ_2 (or ϕ_0 , ϕ_1 and ϕ_s) - these parameters are independent of concentration. Equation 2.4.2 has one parameter which depends on temperature, pressure, and concentration, but not molecular weight this parameter deals with interactions between solvent molecules and polymer molecules. According to Konigsveld et al.[48] this equation is good at explaining the essential aspects of liquid - liquid equilibrium polymer systems, but there are discrepancies between the measured volume ratios of separated phases and those predicted by equation 2.4.2 with a

molecular weight independent parameter. Equation 2.4.4 also has one parameter which deals with interactions between the polymer species A and B. Sariban and Binder[54] identify three assumptions in equation 2.4.4. First, any correlations in the occupancy probability of lattice sites are neglected giving the quadratic term $\chi\phi_A\phi_B$ (χ is a Flory-Huggins parameter). This is a mean field approach, believed to be fairly accurate. The second assumption lies with the entropy term, in that excluded volume restrictions are ignored. The third assumption is with the relation between χ and the nearest neighbour pair energies ε_{AB}, ε_{BB}, and ε_{AA} written as

$$\chi = \frac{z(2\varepsilon_{AB} - \varepsilon_{AA} - \varepsilon_{BB})}{2kT} \qquad 2.4.5$$

Sariban and Binder use a Monte-Carlo calculation as a test of the Flory-Huggin theory.

The parameters χ and g are of such importance because if you know these parameters and how they change with temperature, concentration, composition, pressure, and molecular weight you can determine whether the polymer system will undergo a phase transition or not, and how far the system is from phase separation. As the properties of a system drastically change once a phase transition has occurred (or indeed in the immediate region of phase separation), such complete knowledge of χ and g (and thus of ΔG^M) is of considerable interest.

ΔG^M is not in itself a very useful entity in determining whether or not phase separation has occurred.

In order to find out whether or not two phases can coexist we need to determine the chemical potential of the components involved. The chemical potential of species A is given as the partial derivative of the Gibbs free energy of mixing (ΔG^M) with respect to the number (or number of moles) of species A present. Two phases can coexist only if the chemical potentials of each component are equal in both phases i.e.

$$\Delta\mu_1'(\phi_1', \phi_2', \phi_s') = \Delta\mu_1''(\phi_1'', \phi_2'', \phi_s'') \qquad 2.4.6a$$

$$\Delta\mu_2'(\phi_1',\phi_2',\phi_s') = \Delta\mu_2''(\phi_1'',\phi_2'',\phi_s'') \qquad 2.4.6b$$

$$\Delta\mu_3'(\phi_1',\phi_2',\phi_s') = \Delta\mu_3''(\phi_1'',\phi_2'',\phi_s'') \qquad 2.4.6c$$

These three equations are equations 7 in Hsu et al[46]. When these three equations are solved for ϕ_0, ϕ_1 and ϕ_s the set of ϕ_i's which result give a curve known as the binodal curve. Hsu et al. solve these three equations with $\Delta\mu_i'$s from Tompa's work[55] and using an iterative routine to minimize an objective function containing the difference between $\Delta\mu_i''$ and $\Delta\mu_i''$. The binodal's which they calculated are presented in their first seven figures of ref. 46, which show the effects of varying the parameters in equation 2.4.3.

Hsu et al's[46] work is designed to examine the effects of having solvents of differing qualities for differing species. They show that it is not the absolute values of the χ_{is}'s which matter, but rather the differences between them which govern the phase diagram. This is especially evident in their fig. 4. It is evident from this that solvents of differing qualities reduce the area of miscibility in the phase diagram.

Hsu et al[46] are motivated partly by Zeman and Patterson[56] who calculate spinodal's showing loops in which the boundaries of phase stability do not reach down to the polymer concentration axis (in this case the blend of polymers is miscible at all concentrations, and it is only when solvent is added that phase separation can occur). Their work shows that it is not only the value of χ_{12} (the polymer-polymer interaction) which determines the phase stability, but also the difference between χ_{1s} and χ_{2s}.

It is timely at this point to say a few words about the spinodal and binodal curves. The spinodal is similar to the binodal in that it is a curve defined by ΔG^M, but the spinodal is defined as the boundary of phase stability as opposed to the line of coexistence. For simple one component systems the spinodal is defined as the point (in phase space) where the second derivative of ΔG^M with respect to concentration reaches zero. In n-component systems the spinodal is defined by the condition that the n by n matrix (U) formed by the n^2 elements of second order partial derivatives of ΔG^M with respect to first one component and then a second component has a strictly zero determinant this is described in Kamide[50] (page 418) with a matrix of this kind written out. The spinodal doesn't provide exactly the kind of

phase information one might wish for, but it is easier to determine experimentally than the binodal, and is used exclusively in DLS (the experimental technique of interest to the author) - the reason for this will become clear later. The spinodal curve and the binodal curve intersect at a point known as the critical point; this point is where phase separation first occurs. The critical point is defined by an additional condition given in a similar manner as the spinodal, except one of the rows of the matrix is substituted with the derivative of the determinant with respect to concentration of species A. Such a matrix (V) is also shown in Kamide[50] (page 419). Solc and Koningsveld[57] use these definitions of spinodal and critical points with a warning against finding fictitious critical points. This warning comes about because there are cases where U = 0 and V = 0, and yet the respective point is not a critical point.

As stated before, the theories based on Flory's lattice model all have a quadratic interaction term. These theories assume a concentration of polymers such that the entire volume of solution is filled with polymers (the semi-dilute to concentrated range). Next, it is assumed that there is no correlation between polymer segments (or rather that there are blobs of correlation length ξ which are not intercorrelated). The resulting equations 2.4.1-2.4.4 have all the interesting variations with temperature, concentration, and polymer length relegated to the parameter g or χ_{ii} or simply χ. Konigsveld and Kleintjens[47] use g (which only models for interactions between total polymer fraction and solvent) in a closed form expression

$$g = \alpha + \frac{\beta_0}{1 - \gamma\phi} \qquad 2.4.7$$

with

$$\beta_0 = \beta_{00} + \frac{\beta_{01}}{T} \qquad 2.4.8$$

This form of g gives a good fit of the concentration and temperature dependence of the interaction parameter as reported experimentally on polystyrene-cyclohexane solutions[47].

They also try to capture the molecular weight (M_W) dependence of g by replacing β_0 by ($\beta_0 + \beta_1$) where β_1 shows a similar temperature dependence as β_1.

As Kamide[50] puts it, χ can be expressed phenomenalogically as a power series of the concentration (equation 2.1 in Kamide[50])

$$\chi = \chi_{00}\left(1+\frac{k'}{x_i}\right)\left(1+\sum_{j=1}^{n} p_i v_p^j\right) \qquad (i = 1, \ldots, m) \qquad 2.4.9$$

Where k' and χ_{00} are functions of temperature, X_i is the molar volume ratio of the i^{th} component to the solvent X_i (roughly equal to the degree of polymerization) and v_D is the total polymer volume fraction. The series in equation 2.4.9 may contain only the term p_1 and still provide enough information about phase separation characteristics[50]. The temperature dependencies of k' and χ_{00} are expressed as (equations 2.5 and 2.6 in Kamide[50])

$$k' = k_0\left(1-\frac{\theta}{T}\right) \qquad 2.4.10$$

and

$$\chi_{00} = a+\frac{b}{T} \qquad 2.4.11$$

where k_0 is independent of T and X_i, and θ is the Flory theta temperature. At this temperature the monomers cease to feel an interaction from other monomers, and the second virial coefficient is zero. Kamide[50] relates the second virial coefficient (see equation 1.2 in Kamide[50]) to χ_0 (equal to $\chi_{00}\{1 + (k'/X_n)\}$) by

$$A_2 = \frac{v^2}{v_0}\left(\frac{1}{2} - \chi_0\right) \qquad 2.4.12$$

the second virial coefficient expresses the chemical potential deviation of the solvent in solution from that in the ideal state. According to Kamide[50] the third virial coefficient must be taken into account for polymer concentrations of just a few percent, and the second virial coefficient for the entire range of concentrations.

The thermodynamic model of Flory has been altered and used by many workers in many slightly different forms. All these forms have an interaction parameter which expresses the energies involved in changing the neighbours of polymer units from other polymers to solvent molecules. Few authors attempt to provide a microscopic basis for the interaction parameter - most are content to leave it as a value which is empirically determined.

The preceding discussion regards the thermodynamics not in the vicinity of the phase separation point, and covers only mean field approaches. In the vicinity of the phase separation point a mean field approach is not valid and critical exponents are used to describe the properties of interest.

Solutions close to the phase separation point are not included in this study.

3

The Properties of Polysaccharides in Solutions

The study of polysaccharide systems is of considerable importance in many areas. These include food science, medical science, and the cosmetics industry. The family of polymers based on simple carbohydrate molecules are known as polysaccharides and come in many differing forms. From tree-like dendrimers to, stiff chains and random coils, they can be charged or neutral overall, they can have complex secondary structures, and form an integral part of the machinery of life itself.

Thus, the study of polysaccharides is both very interesting and very complex. Though a detailed description of the many polysaccharides is beyond the scope of this work, a detailed description of the polysaccharides used in this study is given. These polysaccharides have been chosen for their similarity to the ideal polymers described in the theories. Specifically, they are required to be linear, flexible, neutral, homopolymers. Needless to say none of the polysaccharides can be expected to conform precisely to this format, given that the manufacture process is biological in nature and is not exactly controlled in this situation. However given the interest in and importance of these complex biological systems, it seems appropriate to try and extend the body of work done on ideal and hybrid systems to ternary mixtures of polysaccharides in the semidilute regime.

3.1 Polysaccharides: Fundamental Properties

The most common simple sugars are described by chemical formulae of $C_6H_{12}O_6$ or $C_5H_{10}O_5$. Without going into chemical detail, these sugars can form ring structures, six membered rings are called pyranose and five membered rings are called furanose. "Carbohydrates: The Sweet Molecules of Life"[58] is an excellent reference which describes the many different configurations available to these pyranose and furanose rings. These rings can bind together via glycosidic linkages (see chapter 8 of the same reference),

forming disaccharides, trisaccharides, oligosaccharide and polysaccharides, the latter having molecular masses of tens of millions g/mol. Each sugar unit can form one, two, or more glycosidic linkages, leading to the possibility of branched polysaccharide structures.
Polysaccharides have many different functions in the natural world - they act as storage materials, structural materials, protective elements, and as part of the immune defence system.

When less than ten residues are linked in a chain the resulting polysaccharide is termed an oligosaccharide. An interesting group of oligosaccharides are cyclodextrins, which contain six, seven or eight sugar rings. Cyclodextrins have the useful property of forming a structure that can contain "guest" molecules which then travel with the cyclodextrins themselves (p 217 of ref. 58).

To emphasize the many different forms polysaccharides can take, some of the most common forms are described tersely. These forms give examples of polysaccharides which are helical, globular, or a twisted ribbon.

Starch is made up of two polysaccharides, Amylose, and Amylopectin. Amylose has a molecular weight of around 10^6 g/mol, has maltose as its monomer, and is linked by (1->4)-alpha-D linkages. Amylose has a helical structure.
Amylopectin has a molecular weight of 10^8 g/mol, the same monomeric form as Amylose, and branching points about every ten maltose units. Amylopectin is globular in shape.
Cellulose (the most abundant polymer on earth) is made up of cellobiose units and has a variable molecular weight. Cellobiose gives the polysaccharide some rigidity, and hydrogen bonding between chains gives more strength to the polysaccharide, making it an ideal component in the structure of many organisms.

3.2 Xanthan

Xanthan is a widely studied bacterial exopolysaccharide - the interest in this polymer is driven chiefly by the food industry in which it is used as a thickening agent to increase the viscosity of solutions, or as a stabilizing agent, for instance in milk products.

Xanthan is an anionic polysaccharide, its primary structure is a linear cellulosic backbone with a O-β-D-mannopyranosyl-(1,4)-O-β-D-glucopyranosyl-uronic-acid-(1,2)-6-O-acetyl-a-D-mannopyranosyl side chain linked at C(3) of every second glucose residue[59].

The structure of Xanthans in both native and renatured forms under various solution salinities and temperatures has been explored[60-63] and its ordered state has been found to be either a semi-rigid helix or two helixes side by side, while its unordered state is a flexible coil[59]. The transition from order to disorder occurs as salinity is decreased or temperature is increased[64].

3.3 Dextran

Dextran is an exocellular microbial polysaccharide which finds applications in medicine where it is used as a blood plasma volume expander, and to produce iron dextran for the treatment of anaemia. Dextran is made up of alpha-D-glucopyronosyl residues, connected mainly through the alpha-1,6 link. However, different linkages are available for bonding and dextran is technically a hyper branched polysaccharide. Dextran is produced by bacteria (typically *Leuconostoc mesenteroids*) and different strains provide dextrans with differing properties in terms of branching density and/or the length of the side chains. Nordmeier provides evidence that branching becomes more pronounced as the molar mass of dextran increases[36]. In this study a low molecular weight sample was chosen to better approximate a linear polymer, with the intention to use it to study ternary polysaccharide solutions using the theory applicable to linear polymers. Recently there has been a detailed study of dextran in different concentration regimes using both static and dynamic light scattering[44, 66, 67].

At lower concentrations dextran was found to be well explained using the available theories. At semidilute concentrations and above, these investigations found a fast diffusion coefficient and a slow diffusion coefficient present in solution.
The self-diffusion coefficients of individual dextran molecules in solution were determined, and found to decrease with increasing concentration. The apparent molecular weight of dextran was also found to increase with concentration - due to association effects.
The conclusions of these studies are presented in more detail in section 6.2.3 of this work

3.4 Pullulan

Pullulan is an exocellular microbial polysaccharide typically obtained by the cultivation of the fungus *Aureobasidium pullulan* on glucose (p462 of ref. 68).
Pullulan is a linear polysaccharide composed of maltotriose units linked by α-D-(1, 6) glycosidic bonds. This polysaccharide is water soluble and biodegradable, and has generated much interest in the cosmetic, food and pharmaceutical industries.

3.5 Guar

Guar gum comes from the seed of the guar plant *Cyamopsis tetragonolobus*. Guar is a neutral linear chain made up of D-mannose units joined by β-D-(1, 4) linkages with random substitutions of D-galactose side chains on approximately every other mannose unit. As the substitutions are random, regions rich in galactose and poor in galactose are formed. These galactose poor regions are less soluble than the galactose rich regions, leading to partially crystalline sections. This leads to cross linking between guar polysaccharides (junction zones) which promotes gelation[69]. In the food industry guar gum galactomannon is used as a thickener, as a stabiliser of ice-cream, and to aid in the spreadability of cheese spreads (p462 of ref. 68). Industrially guar is mainly used in paper production and the mining industry. The structure of guar in solution has recently been investigated by Gittings et.

al.[70, 71]. The main conclusion by these authors is that the behaviour of guar in solution is dominated by the formation of aggregates.

3.6 Sodium Caseinate

Sodium Caseinate appears last in this section as it is not a polysaccharide at all, rather it is a protein. Casein is the most abundant protein present in milk solutions and forms roughly spherical, stable colloidal particles known as casein micelles. Sodium caseinate is a commercially available, water soluble form of casein that is widely used in the food industry for its functional and sensory properties. Sodium caseinate is used, amongst other things, to stabilize fat globules in cream liqueurs, as an emulsifier, and as a thickener.

Sodium caseinate is a less than well-described biopolymer, being a collection of different proteins. Three quarters of the protein making up sodium caseinate is in the form of α_{s1}-Casein and β-casein[65]. Both these proteins exist in solution as linear disordered chains containing about 200 amino acid residues, with about 20 residues negaitvely charged.

It should be emphasised that Na-CN is a protein, not a polysaccharide.

4

The Theory of Light Scattering

Light scattering is widely used to study the properties of polymeric solutions. Its main application is to transparent solutions in which the light is scattered once, although multiple scattering solutions have also been studied, notably in the recently introduced diffusing wave spectroscopy technique. It is a non invasive technique which is widely used to characterize the properties of macromolecules in solution. Light scattering from dilute transparent solutions comes in two varieties, static and dynamic. Static light scattering deals with the time average intensity of the scattered light, and is related to the density variations in the solution. In a binary solution the quantities gathered using this approach give a measure of the interactions between the polymers, and for instance the molecular masses. The shapes of individual polymers can also be approximated using this technique. Static light scattering is mainly applied in the dilute regime where the interactions between the polymers are minimal.

Dynamic light scattering measures the variation of the scattered light intensity with time and it can be used to study how the fluctuations in solution are correlated over time. The self diffusion coefficients and the hydrodynamic radius of the macromolecules can be determined with this technique.

Light is described classically as an electromagnetic field propagating through space. The oscillating electric field induces a polarization of the atoms encountered by the field. In turn these polarized atoms serve as secondary sources of radiation, scattering the light. The properties of the scattered light such as intensity, angular distribution, polarization, and frequency shift are determined by the properties of the material doing the scattering.

There are many works available which describe the development of the concepts used here[72-76]. These use Maxwell's equations to determine the scattered field in terms of fluctuations in the dielectric constant. If the fluctuations in the dielectric constant (or the

polarization) of the solution under investigation can be determined theoretically (in terms of some molecular parameters) then the scattered light can be used to determine the parameters under investigation.

4.1 The Scattered Field

Without reproducing Maxwell's equations here, the foundations of light scattering are presented as related to intensity autocorrelation functions (the experimentally determined quantity in this work). The summary of light scattering presented here follows that of chapter 3 in ref. 73.

Laser light has a narrow distribution of frequencies and is well described by the plane wave approximation

$$\mathbf{E}_{\mathrm{INC}}(\mathbf{R}, t) = \mathbf{n}_i E_0 \exp[i(\mathbf{k}_i \cdot \mathbf{R} - \omega_i t)] \qquad 4.1.1$$

In this work $\mathbf{E}_{\mathrm{INC}}$ represents the electric field of the incident laser light, $\mathbf{n}_i$ is a unit vector in the direction of the incident electric field, $\mathbf{k}_i = (\omega_i / c)\hat{\mathbf{k}}_i$ is the wave vector (with $\hat{\mathbf{k}}_i$ the direction the wave propagates), and ω_i is the frequency of the wave. The dielectric constant in the medium under illumination is given by

$$\varepsilon(\mathbf{r}, t) = \varepsilon_0 \mathbf{I} + \delta\varepsilon(\mathbf{r}, t) \qquad 4.1.2$$

where $\mathbf{I}$ is a second rank unit tensor and $\delta\varepsilon(\mathbf{r}, t)$ is the dielectric constant fluctuation tensor at $\mathbf{R}$ and t. Using these two equations in conjunction with Maxwell's equations, the amplitude of the light scattered by $\mathbf{E}_{\mathrm{INC}}$ at a large distance R from the scattering volume v, with polarization $\mathbf{n}_f$, propagation vector $\mathbf{k}_f$ and frequency ω_f, a result is given by[73]

$$E_S(R, t) = \frac{E_0}{4\pi R \varepsilon_0} \exp ik_f R \int_v d^3r \exp i(\mathbf{q} \cdot \mathbf{r} - i\omega_f t)$$

$$[\mathbf{n}_f \cdot [\mathbf{k}_f \times (\mathbf{k}_f \times (\delta\varepsilon(\mathbf{r}, t) \cdot \mathbf{n}_i))]] \qquad 4.1.3$$

In this equation the scattering vector $\mathbf{q} = \mathbf{k}_i - \mathbf{k}_f$ is a result of the experimental geometry. In this work we are interested in the case of quasi elastic scattering, where $|\mathbf{k}_i| = |\mathbf{k}_f|$ - so $q^2 = (4\ \pi\ n/\lambda)^2 \sin^2(\theta/2)$, where n is the refractive index of the solvent, λ is the wavelength of the incident light and θ is the scattering angle. The scattering system and geometry are shown in fig. 4.1.

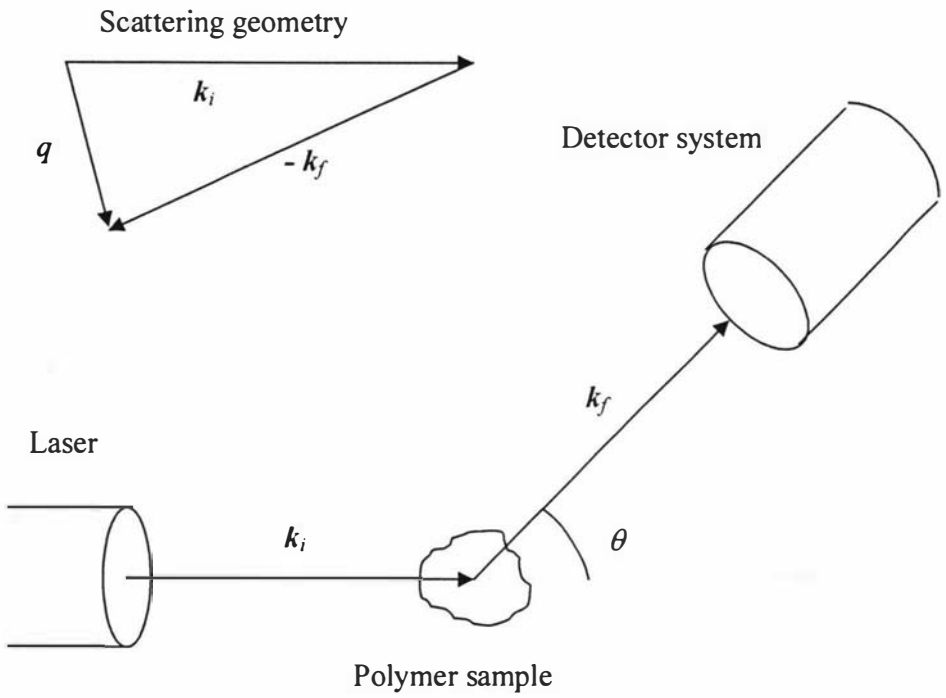

Figure 4.1 Scattering system and geometry

Equation 4.1.3 may be simplified if we take the Fourier transform of the dielectric fluctuations

$$\delta\varepsilon(\mathbf{q}, t) = \int_v d^3 r \exp i(\mathbf{q} \cdot \mathbf{r}) \varepsilon(\mathbf{r}, t) \qquad 4.1.4$$

After some manipulation the resulting expression for the scattered field is

$$E_S(R, t) = \frac{-k_f^2 E_0}{4\pi R\varepsilon_0} \exp i(k_f R - \omega_f t)\, \delta\varepsilon_{ij}(\mathbf{q}, t) \qquad 4.1.5$$

where

$$\delta\varepsilon_{ij}(\mathbf{q}, t) = \mathbf{n}_f \cdot \delta\boldsymbol{\varepsilon}(\mathbf{q}, t) \cdot \mathbf{n}_i \qquad 4.1.6$$

the latter is the component of the dielectric constant fluctuation tensor along the initial and final polarization directions. From equation 4.1.5 it is seen that the electric field of the scattered light is dependant on the fluctuations in the dielectric constant.

4.2 Auto Correlation Functions

The properties of matter in bulk have traditionally been described in terms of statistical mechanics because the large number of particles involved in macroscopic experiments means that ensemble averages are appropriate. A simple first order statistical measure is the time average

$$\overline{A} = \lim_{T\to\infty} \frac{1}{T} \int_0^T dt\, A(t) \qquad 4.2.1$$

We are interested in ergodic systems in which the time averages are equal to ensemble averages so

$$\langle A \rangle = \overline{A} \qquad 4.2.2$$

$A(t)$ is the measured time dependant bulk property in an equilibrium system, and is assumed to be stationary, meaning that the average described by equation 4.2.2 is independent of when the measurement starts.

A more interesting statistical measure is the second order autocorrelation function. This measure relates the signal at time t_0 with the signal measured at a later time $t_0 + \tau$ (a delay time of τ). Typically a measured signal varies in such a way that with sufficiently small delay times the signal will not change appreciably and if an average over start times t_0 is taken a positive value will be found. That is to say that for sufficiently small delay times the signal is correlated with itself.

As the delay time increases the signal is more likely to be further from its initial value and when an average is taken over start times a smaller value is found.

Assuming a stationary process the autocorrelation function of $A(t)$ is given by

$$< A(0)A(\tau) >= \lim_{T\to\infty} \frac{1}{T} \int_0^T dt\, A(t)A(t+\tau) \qquad 4.2.3$$

With $\tau = 0$, this gives an average of the square of A.

4.3 Intensity Autocorrelation Functions, Density Fluctuations and the Seigert Relationship

Taking the autocorrelation function of $E(R, t)$ from equation 4.1.5, the following result is obtained

$$<E_S^*(R, t)\, E_S(R, t+\tau) > = \frac{k_f^4 E_0^2}{16\pi^2 R^2 \varepsilon_0^2} < \delta\varepsilon_{if}(\mathbf{q}, 0)\, \delta\varepsilon_{if}(\mathbf{q}, \tau) > exp\ -i(\omega_f t) \qquad 4.3.1$$

This is called the field autocorrelation function and is usually referred to as $G^{(1)}(\tau)$ if unnormalized - when normalized it is written as $g^{(1)}(\tau)$ and it ranges between unity at $\tau =$ [illegible] to zero.

The electric field fluctuates at a rate outside a measurable range, so instead the quantum nature of light is exploited by counting the photons scattered. The photon count is proportional to the intensity, which is related to the electric field by

$$I(t) \propto E^*(t)\, E(t) \qquad 4.3.2$$

The autocorrelation function of the intensity is a measurable quantity and, if the statistics of the scattered light are Gaussian, it can be related to the field autocorrelation function by the well known Seigert relationship[76]. If

$$G^{(1)}(\tau) = \langle A(0)\, A^*(\tau) \rangle \qquad 4.3.3$$

is the first order correlation function and

$$G^{(2)}(\tau) = \langle |A(0)|^2\, |A(\tau)|^2 \rangle \qquad 4.3.4$$

is the second order correlation function, then

$$G^{(2)}(\tau) = G^{(1)}(0)^2 + |G^{(1)}(\tau)|^2 \qquad 4.3.5$$

For normalized functions this equation is written as

$$g^{(2)}(\tau) = 1 + |g^{(1)}(\tau)| \qquad 4.3.5a$$

and $g^{(2)}(\tau)$ ranges from 2 to unity. This means that the field autocorrelation can be found if the intensity autocorrelation function can be obtained. Equation 4.3.5a is the Seigert relationship - using it we find

$$\sqrt{g^{(2)} - 1} = g^{(1)}(\tau) = \beta G^{(1)}(\tau) \qquad 4.3.6$$

β is a normalization parameter determined by the experimental setup. The left hand side of equation 4.3.1 can be obtained by light scattering experiments using an autocorrelator and applying the Seigert relationship to the measured second order (or intensity) autocorrelation function, while the right hand side contains information about the wavelength of light used ($k_f \propto 1/\lambda$), the distance of the scattering volume to the detector R, the field amplitude E_0, and the autocorrelation function of the dielectric constant fluctuations $<\delta\varepsilon_{if}(\mathbf{q}, 0)\ \delta\varepsilon_{if}(\mathbf{q}, t)>$.

4.4 A Molecular Approach to Density Fluctuations

The preceding discussion has focused on the dielectric constant fluctuations from a continuous media. It is instructive to take a molecular approach in order to relate the problem to physical quantities such as the number of molecules, temperature, pressure, and volume.

If the induced dipole moment from the scattering particle (labelled j) is,

$$\mu(t) = \alpha_j(t)\,\mathbf{E}(t) \qquad 4.4.1$$

with α_j the polarizability of the j^{th} particle, the polarizability density from point particles at positions $\mathbf{r}_j(t)$ is

$$\delta\alpha(\mathbf{r}, t) = \sum_j^N \alpha_j(t)\,\delta\left(\mathbf{r} - \mathbf{r}_j(t)\right) \qquad 4.4.2$$

The total amplitude detected from the collection of N molecules in the scattering volume is

$$\delta\alpha(\mathbf{q}, t) = \sum_j^N \alpha_j(t)\exp\, i\mathbf{q}\cdot\mathbf{r}_j(t) \qquad 4.4.3$$

which is the spatial Fourier transformation of the polarizability density $\delta\alpha(\mathbf{r}, t)$. The intensity may then be expressed as the autocorrelation function of $\delta\alpha(\mathbf{q}, t)$

$$I(\mathbf{q},t)=\left\langle \delta\alpha^{*}(\mathbf{q},0)\delta\alpha(\mathbf{q},t)\right\rangle \qquad 4.4.4$$

If we consider a scattering volume in which the scattering objects are all spherical particles, then $\alpha_j(t)$ is identical for all j, and the sum in equation 4.4.2 is simplified to the constant α multiplied by $\sum_j \delta\left(\mathbf{r}-\mathbf{r}_j(t)\right)$ which is the instantaneous number density $\rho(\mathbf{r}, t)$ at point $\mathbf{r}$ and time t. It is clear that the fluctuations in density may be related to the light scattered. The measured intensity autocorrelation function therefore contains information regarding the fluctuations in density, which in turn can be related to the displacement of the molecules in solution and the interactions between them. Such relationships have been explored in chapter 2.

4.5 CONTIN

The resolution of the measured autocorrelation functions into a sum of exponential decay rates is an ill posed problem. CONTIN is a program written by Provencher[77, 78]. CONTIN, or some procedure using a modified form of CONTIN, is universally used to solve this kind of problem in dynamic light scattering experiments. A brief description of CONTIN is given here.

CONTIN can be used to solve Fredholm integral equations of the first kind

$$y_k = \int_a^b K(g,t_k)s(g)dg + \sum_{i=1}^{N_L} \beta_i L_i(t_k) \qquad \text{k} = 1, ..., N_y \quad 4.5.1$$

The function $K(g,t_k)$ is specified for a given problem, t_k are known, and $s(g)$ is to be estimated. The optional sum over known $L_i(t_k)$ and N_L the unknown β_i, can be used to allow for a constant background term to be included by setting the $L_i(t) = 1$ and $N_L = 1$.
In DLS such a term can be used to represent the presence of long term correlations outside the window examined by the autocorrelator used. This is often referred to as a dust term.

In dynamic light scattering applications eqn 4.5.1 becomes

$$g^{(1)} = \int_0^\infty e^{-\Gamma t} A(\Gamma) d\Gamma \qquad 4.5.2$$

CONTIN converts this to a set of linear algebraic equations by numerical integration of eqn 4.5.1

$$y_k = \sum_{m=1}^{N_g} c_m K(g_m,t_k)s(g_m)dg + \sum_{i=1}^{N_L} \beta_i L_i(t_k) \qquad \text{k} = 1, ..., N_y \quad 4.5.3$$

where c_m are the weights of the quadratic formula. A set of $s(g)$ is then found for the N_g grid points g_m.

The ill posed nature of eqn 4.5.1 means that even for arbitrary levels of noise present in y_k there exist many solutions $s(g)$ which fit the y_k to within the noise level.

If eqn 4.5.3 is written

$$y_k = \sum_{j=1}^{N_x} A_{kj} x_j \qquad 4.5.4$$

then there will be a solution $s(g)$ which will be the least squares fit, such that

$$VAR = \sum_{k=1}^{N_y} w_k \left(y_k - \sum_{j=1}^{N_x} A_{kj} x_j \right)^2 \qquad 4.5.5$$

is a minimum for the chosen x_j, and w_k are weights which can be assigned. This method proves unreliable in finding the correct solution.

Instead CONTIN uses a regularized solution, which is the set of x_j that minimizes

$$VAR + \alpha^2 \sum_{k=1}^{N_y} \left(r_i - \sum_{j=1}^{N_x} R_{ij} x_j \right)^2 \qquad 4.5.6$$

subject to the constraints

$$\sum_{j=1}^{N_x} D_{ij} x_j \geq d_i, \qquad i = 1, \ldots, N_{\text{ineq}} \qquad 4.5.7$$

$$\sum_{j=1}^{N_x} E_{ij} x_j \geq e_i \qquad i = 1, ..., N_{eq} \qquad 4.5.8$$

The arrays D, E, d, and e are specified by the user, and allow one to use prior knowledge about the system to rule out some solutions - for instance that the solution be non negative.

The second term in eqn 4.5.6 is called the regularizer and is determined by setting the values r_i, R_{ij} and α. These values are chosen either on the basis of a priori knowledge about the system at hand or using the principle of parsimony. Generally, this means choosing a solution which is most smooth.

4.6 CONTIN multiq

The distribution of amplitudes $A(\tau)$ in equation 4.5.2 contains no information regarding the scattering vector q, if the distribution $A(\tau)$ has some known variation with q or if the distribution is expected to come in the form of a sum of q dependent and q independent modes. This information can be used to combine data from a range of scattering angles and used simultaneously to determine $A(\tau)$.

CONTIN has been modified to exploit this information[79] - an approach also taken by Buttgereit et al.[80].

For instance, if the distribution of amplitudes is expected to be a sum of q independent contributions and q^z contributions, then the unnormalized first order correlation function may be written

$$\beta(q)\hat{g}_1(t;q) = \int_0^\infty q^z A_r(\tau) e^{-t/\tau} d\tau + \int_0^\infty A_d(D) e^{-q^2 Dt} dD \qquad 4.6.1$$

where $\beta(q)$ are the unknown scale factors due to the experimental setup, and $\hat{g}_1(t;q)$ are first order autocorrelation functions at different scattering angles. Diffusive modes vary

linearly with q^2 and so to detect a sum of relaxation (q-independent) modes and diffusive modes, z is set to 2. $A_r(t)$ and $A_d(t)$ are q independent.

Equation 4.6.1 is discretized to obtain

$$\hat{g}_1(t;q_i) = \sum_{j=1}^{N_{grid}} q_i^2 \tau_j A_r(\tau_j) e^{-t/\tau_j} d\tau + \sum_{j=1}^{N_{grid}} D_j A_d(D_j) e^{-q_i^2 D_j t} d\tau + C_i + [1-\beta(q_i)]\hat{g}_1(t;q_i) \qquad 4.6.2$$

where i =1,....,N_{ACF} and N_{ACF} is the number of autocorrelation functions taken at different scattering values. C_i are the usual dust terms. (1- β_i) and C_i are treated as linear parameters to be estimated. CONTIN multiq can be set to provide a dust term for each angle, a dust term for each set of angles, or no dust term at all. One data set is set as a reference and the other data sets are scaled with β_i to match the reference data.

The consistency of the assumptions made in eqn 4.6.1 are tested by the incompatibility ratios

$$R_i = \frac{VAR_i^{global}}{VAR_i^{single}} \qquad i = 1,...,N_{ACF} \qquad 4.6.3$$

where

$$VAR = \sum_{k=1}^{N_{data}} \frac{g_i(t_k) - \hat{g}_i(t_k)}{\sigma_k^2} \qquad A(\tau) \geq 0 \qquad 4.6.4$$

σ_k is proportional to the standard deviation of the noise in the data point $g_1(t_k)$. Where a global fit is being used, N_{data} is the total number of data points in all correlation functions. R_i gives a measure of the relative fit of each data point to the global hypothesis, when all the R_i are less than 1 the data are completely consistent with the assumptions used in equation 4.6.1.

Both CONTIN and CONTIN multiq are available for download at www.provencher.de.

The output from CONTIN multiq in its default configuration comes in the form of two grids, one giving amplitudes of diffusive rates and one giving amplitudes for non-diffusive rates.

5

Experimental Set-Up

In order to extract dynamical information about ternary polymer solutions a laser is used to scatter light from a sample volume, the photons scattered are counted using a photo multiplier tube and the resulting signal must be autocorrelated in order to extract information such as the hydrodynamic radius of a polymer in solution. The apparatus used has been described previously[81]. This chapter describes the experimental equipment used in this work.

5.1 The Experimental Set-Up

A vertically polarized argon ion laser (spectra physics 165) operating at 488 nm was used as a light source. The sample was kept at 25°C in a precision devices 4300 spectrometer. The full homodyne intensity autocorrelation function of the scattered light was obtained using either the autocorrelator designed by Yi as part of his PhD project[82] or a correlator.com Flex 990EM-12 multiple tau auto/cross-correlator.

The work on the sodium caseinate/xanthan ternary solutions was done using Yi's autocorrelator - however, this autocorrelator stopped working up to specification, the final 64 channels no longer giving any output.

The work on the guar/dextran and the dextran/pullulan ternary solutions was done using the correlator.com Flex 990EM-12 multiple tau auto/cross-correlator.

Initially a pinhole set up was used to collect scattered light for a photomultiplier tube (PMT) attached to the spectrometer. A diagram of the experimental apparatus is shown in fig. 5.1.

In the later work on Dextran and Pullulan ternary mixtures a single mode fibre optic cable was used to collect the scattered light. This modification was made to better ensure the light detected came from a single coherence area, and is inspired by the work done by Ricka[83] and Gisler et al.[84].

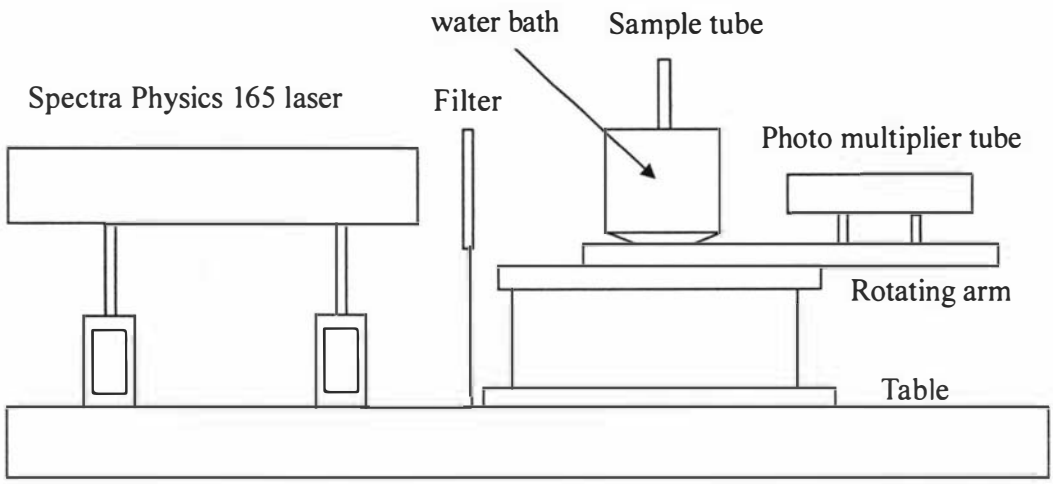

Figure 5.1 DLS experimental apparatus

6

Results

Three different ternary polymer solutions have been investigated. The first of these is the ternary system of sodium caseinate (Na-CN) and xanthan. Sodium caseinate and xanthan are both biopolymers of considerable commercial interest and it was seen as instructive to examine this system even though the theories outlined are not expected to work for this system.

The next is the guar and dextran system. Guar and dextran were chosen both because of their commercial applications and because they are both observed to behave like flexible coils under the experimental conditions explored here. This system was seen as being a reasonable candidate for testing the Sun and Wang theory.

The last is the dextran/pullulan system. Pullulan is seen as an interesting biopolymer to the cosmetic and food industry as it is water soluble and biodegradable, as yet its application is limited. Dextran and pullulan were seen as ideal biopolymers to test the theory.

These solutions have all been studied at 25°C and the concentrations have been chosen to lie in the semidilute regime to maximize the validity of the theories used.

The work on Na-CN and xanthan has been published and is appended to this thesis as appendix A. The published work on Na-CN and xanthan is not couched in terms of the Sun and Wang theory and additional work is presented here for comparison with the theory. The guar and dextran work has been published and compared with the theory; the reader is referred to appendix B for details about the results of that work.

The work on dextran and pullulan is presented here after the Na-CN and xanthan work.

The food industry is mainly concerned with biopolymers in aqueous solution, and so the process of matching solvents to polymers is constrained. The determination of the self diffusion coefficients and the cross second virial coefficient for two polymers of arbitrary molecular weights, solvent qualities, and optical contrasts is the main advantage of Sun and Wang's theory.

Throughout this work the composition (x), as used in section 3 of chapter 2, is defined in a different way for each system. In the Na-CN/xanthan work x refers to the number of monomers of Na-CN to total monomer number; in the guar/dextran work x is the monomer fraction of guar to total monomer number; and in the dextran/pullulan work x is the monomer fraction of dextran to total monomer number. Conversions from weight fractions (w) to monomer fractions were done using

$$x = \frac{w}{w + (1 - w)\frac{m_1}{m_2}} \qquad 6.1$$

where m_1 and m_2 are the monomer molecular weights of polymer 1 and 2 respectively.

6.1 Sodium Caseinate and Xanthan

The materials and methods, and some of the experimental data for this system are presented in appendix A, while additional data is presented here and discussed in relation to the Sun and Wang theory. It should be noted that in food systems the ratio of Na-CN to xanthan would be 10 to 100. In this work the ratio varies from 1:3 to 3:1, these ratios were chosen simply to provide an even range of composition values from zero to one.

Sun and Wang's theory relies on a large number of experimentally determined parameters. One of these, the relative monomer masses m_1/m_2, has no unique value when dealing with proteins (as they have no one base unit), therefore in order to make use of this theory here, m_1 is set equal to m_2. As this system was chosen mainly to gather data on a commercially interesting solution - rather than its value in testing the theory at hand - no attempt was made to refine the value of m_1/m_2 , such as using the average value of the amino acids comprising Na-CN as the value of m_1. The value for the refractive index increment of xanthan in water has been taken as 0.143 mL/g, and that of Na-CN in water is set as 0.181 mL/g. The values for the molecular weights, second virial coefficients, and radii of gyration

of xanthan and Na-CN have been experimentally determined using static light scattering (see table 6.1).

The polydispersity of these biopolymers is unknown.

Table 6.1 The parameters of xanthan and Na-CN determined by static light scattering

	M_w (g mol^{-1})	A_2 (m^3 mol kg^{-2})	R_g (nm)	dn/dc × 10^3 (m^3 kg^{-1})
Na-CN	3.2×10^6	-1.0×10^{-4}	78	1.8×10^{-1}
Xanthan	4.1×10^6	2.7×10^{-4}	150	1.4×10^{-1}

The polymers used here are larger than used by most dynamic light scattering experimenters. Generally linear polymers such as polystyrene or polymethlymelthacrylate fractions that are an order of magnitude smaller are used and some studies on xanthan have concentrated on lower molecular weight fractions[92].

The Sun and Wang theory, as summarized in section 3 of chapter 2, contains the scattering vector q through the particle form factor P. This form factor also contains the radius of gyration, R_g, associated with the scattering molecule. In fact it is the product of the two quantities q and R_g which determine P, if $u = (qR_g)^2$ then $P(u) = 2(e^{-u} - 1 + u)/u^2$. This is the Debye formula and assumes a random coil approximation.

The product qR_g here is approximately 3.8 for xanthan and 1.9 for Na-CN and the values of P_1 and P_2 at a scattering angle of 90° given by this method are 0.4 and 0.13 respectively. The solutions D_{s1}, D_{s2} and $A_{2,12}$ are dependent on these values.

This work uses xanthan mixed with Na-CN in water with 0.1 M NaCl and at 25°C. The pH of the Na-CN/xanthan solutions were adusted to 7. The ionic concentration was chosen to be as high as possible to screen out the electrostatic forces, while low enough that the xanthan would be in its disordered state[93] - a random coil configuration. Milas et al.[93] suggest that a ratio of xanthan concentration to salt concentration of 2 or less is needed to screen out the electrostatic interactions (they used NaBr as the salt). At the highest xanthan concentrations used in this study the ratio of xanthan concentration to salt concentration is 1.125×10^{-2}, suggesting that the electrostatic interactions are fully screened.

Measurements were taken at 90° and Sun and Wang's theory is fitted to the two exponentials present in the field autocorrelation function obtained from these ternary solutions.

While it is not expected that this theory will accurately describe the system at hand, this work follows the approach of others in applying theories of semi-flexible neutral polymers to xanthan, which is an anionic polymer.

6.1.2 Results: Sodium Caseinate and Xanthan

The relative amplitude of the slow eigenmode to the fast eigenmode is shown in fig. 6.1 the slow mode dominates at all concentrations and compositions present in this study, and the relative amplitude is always greater than 0.7. Due to the small fast mode amplitude, and the relatively high error in the fast mode (often 20% or more as reported by CONTIN), there is a large error in the relative amplitude. No trend in the fast mode can be discerned over the total polymer concentration.

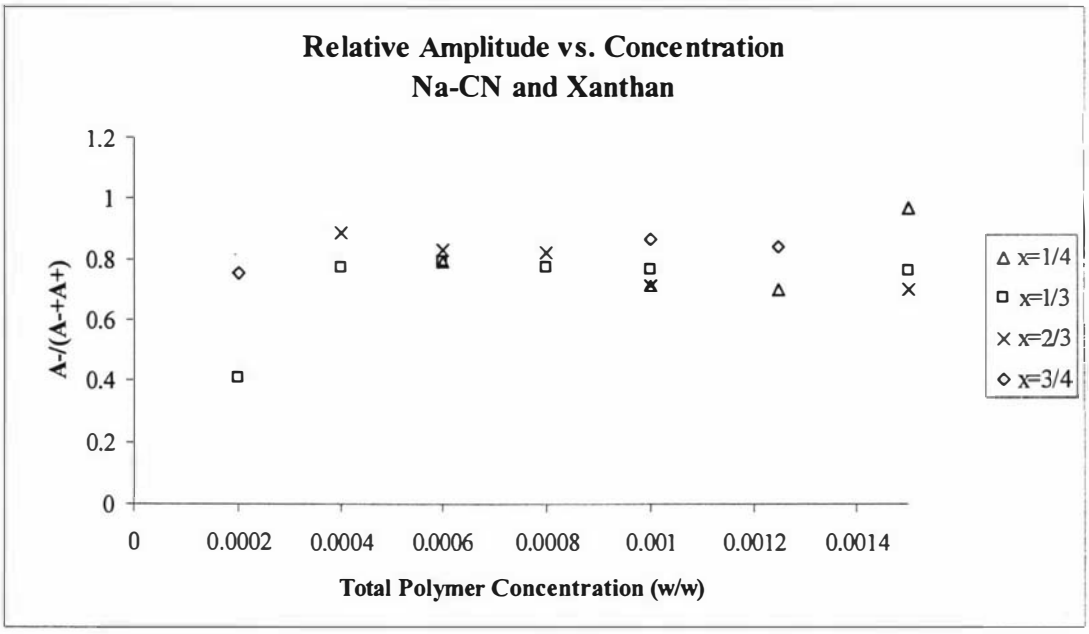

Figure 6.1 The relative amplitude of the slow diffusion coefficient in the Na-CN/xanthan ternary solutions

The small amplitude of the fast mode made the accurate determination of its diffusion coefficient more difficult than that of the slow mode and figures 6.2 and 6.3 show that the fast diffusion coefficient is more scattered than the slow diffusion coefficient. The data points at the smallest total polymer concentration overlap each other and it is not easy to discern a clear trend in the higher concentration data points. These graphs show the error as give by CONTIN, this error is statistical in nature and is a conservative estimate. These

errors tend to be so large that they obscure the data, and they have not been shown on subsequent graphs

The high composition (x = 3/4) data had more points with unreasonably large error values and only two points have been shown, these have an error of about 40% in the fast mode.

In these data, neither the fast nor the slow diffusion coefficient is seen to have a strong concentration or composition dependence.

The results of the Sun and Wang theory are displayed in figures 6.4 and 6.5. Fig. 6.4 shows a combined log-log plot of D_{s1} (The self-diffusion coefficient of the Na-CN) and D_{s2} (the self-diffusion coefficient of xanthan) vs. total concentration. Fig. 6.4 illustrates the relative values of D_{s1} and D_{s2} for the different compositions (x = 1/4, x = 1/3, x = 2/3 and x = 3/4).

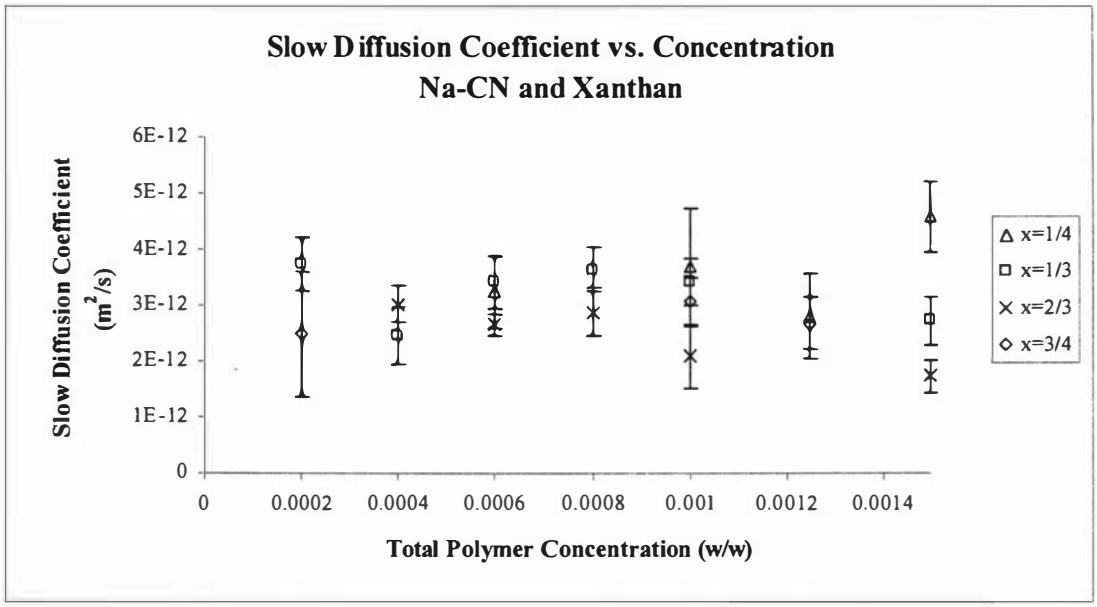

Figure 6.2 The slow diffusion coefficient vs. concentration in the Na-CN/xanthan ternary solutions

D_{s1} does not appear to vary systematically with composition, and decreases with concentration for all but the highest composition. Again, from these data it is only possible to estimate the value of D_{s1} at the concentrations and compositions used.

The average values of D_{s1} and D_{s2} are 7×10^{-12} m^2s^{-1} and 7×10^{-13} m^2s^{-1}. These values can be compared with those found by Sun and Wang on more ideal systems[31-33], for instance

they present values of around 4 × 10^{-12} m^2s^{-1} and 2 × 10^{-11} m^2s^{-1} for the self-diffusion coefficients of polystyrene and polyisoprene respectively. These values are an order or two of magnitude larger than the values here. This would be expected, as the radii and molar mass of the polymers used here are much larger than those used by Sun and Wang.

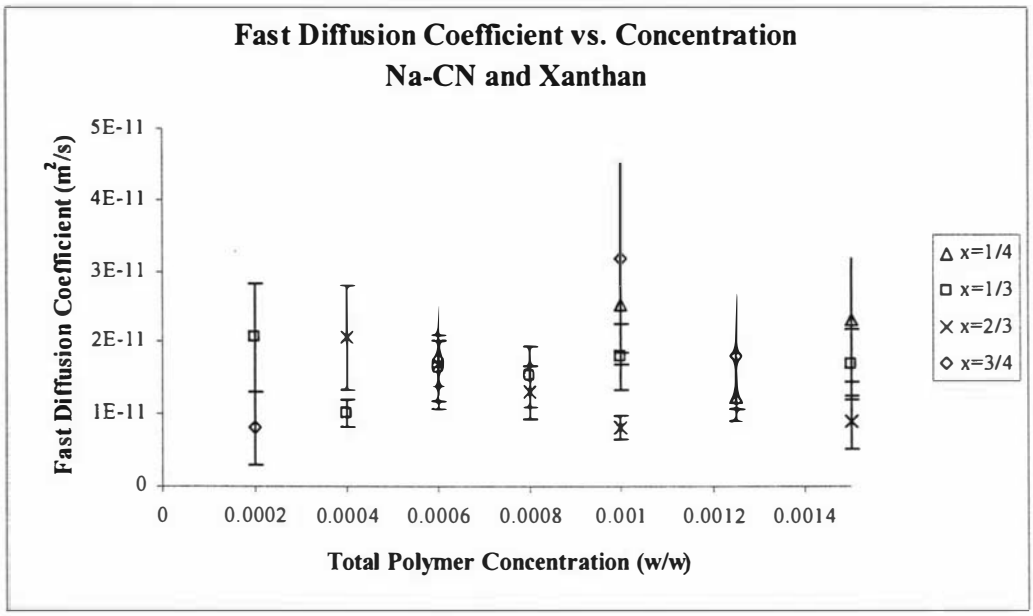

Figure 6.3 The slow diffusion coefficient vs. concentration in the Na-CN/xanthan ternary solutions

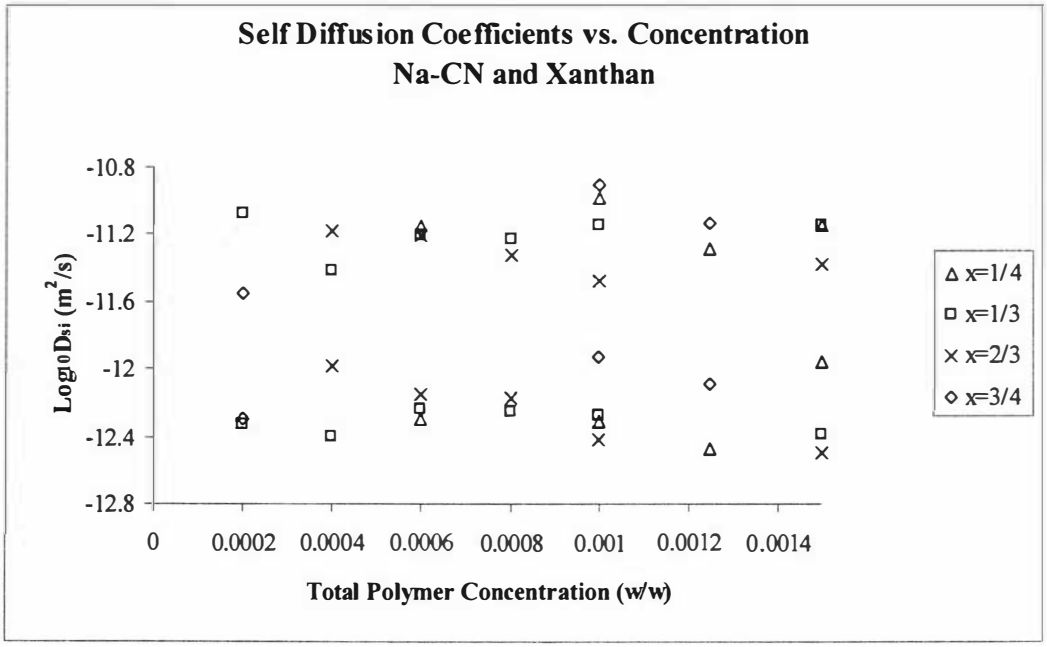

Figure 6.4 A log-log plot of the self diffusion coefficients vs. concentration in the Na-CN/xanthan ternary solutions

The variation of $A_{2,12}$ with concentration is shown in fig. 6.5 - for all compositions this quantity is negative and close to zero, about –0.001. This value is used to determine χ_F, and these values are shown in fig. 6.6 - they suggest that the interaction between unlike polymer segments is small and attractive. χ_F becomes less negative as concentration increases, implying a decrease in interaction with increasing concentration.

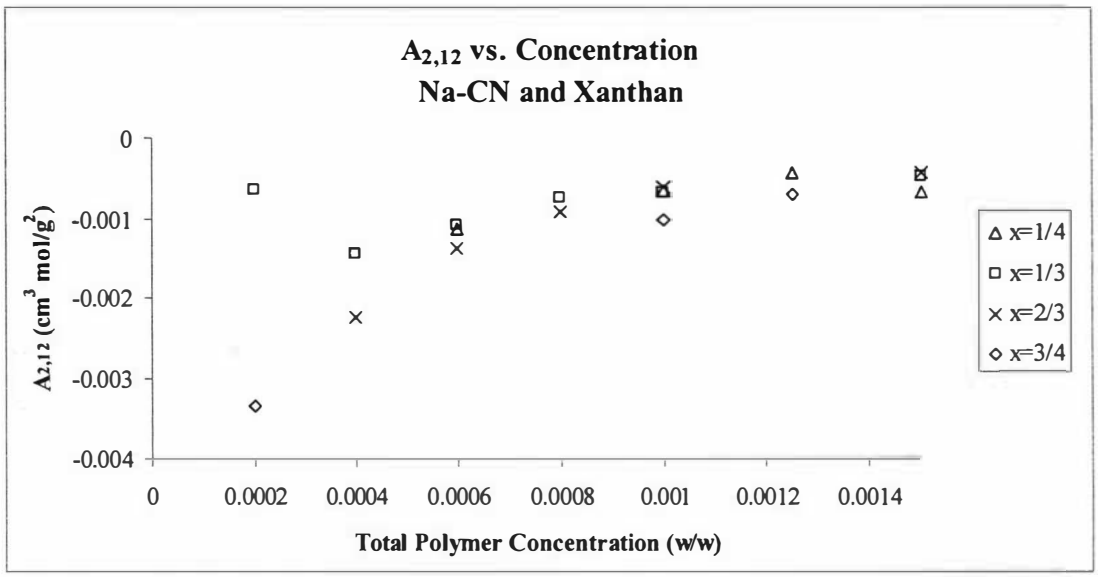

Figure 6.5 The cross second virial coefficient vs. concentration in the Na-CN/xanthan ternary solutions

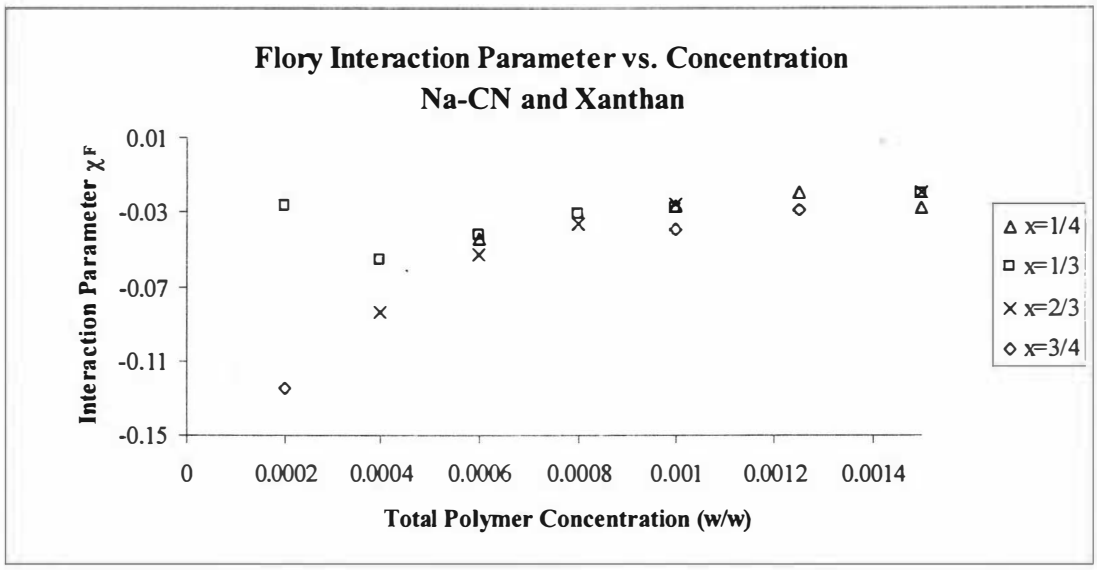

Figure 6.6 The Flory interaction parameter vs. concentration in the Na-CN/xanthan ternary solutions

As already, mentioned the self-diffusion coefficients are plotted against concentration as a log-log plot, although the data are not good enough to read much into the exponents. However, fits have been forced and the exponent in $D_s \propto C^B$ determined. These values are shown in table 6.2 for both self-diffusion coefficients at every composition. The exponents are mentioned for completeness only, as the data was over too small a range and are too scattered to provide meaningful results of this nature.

Table 6.2 The exponents of D_{si} calculated for the Na-CN and xanthan solutions for each composition

	$x = 1/4$	$x = 1/3$	$x = 2/3$	$x = 3/4$
D_{s1}	-0.13 ± 0.15	0.02 ± 0.13	-0.46 ± 0.08	-2.4
D_{s2}	0.46 ± 0.24	0.03 ± 0.08	-0.91 ± 0.06	-1.8

This work has attempted to use the theory of Sun and Wang to determine the self-diffusion coefficients of the biopolymers xanthan and Na-CN in ternary solutions with water as the solvent.

The system used here was far from ideal. Unlike most other experiments, $qRg > 1$, so strictly internal modes should be accounted for - it is assumed that they occur on time scales outside the range of this experimental setup. This seems justified given that only two modes are seen for most samples, although some have a third mode that is slow, has low amplitude and is broad.

Further study at higher concentrations may provide a clearer relationship between the self-diffusion coefficients and concentration. Improved data are needed to discern a trend in D_{s1} and D_{s2} with composition.

6.1.3 Conclusion

In summary, it has proved difficult to gather reliable, precise data on this system (especially at high Na-CN compositions) using this experimental set-up. However, while the self-diffusion coefficients can only be considered order of magnitude estimates, they seem reasonable in relation to values reported by Sun and Wang on smaller radii polymers.

Xanthan is a well-studied biopolymer, however its wormlike nature and negative charge means a modified theory is needed to describe its dynamical behaviour in solution with other bioploymers. Sodium caseinate is not a standard polymer in that its make up is different for different sources, and it has no monomers as such. Again it should be noted that Na-CN, unlike the other biopolymers used in this study, is a protein, not a polysaccharide. It is definitely stretching the theory to use it on such a biopolymer, and, given the difficulty experienced in collecting sufficiently precise data at high Na-CN compositions, this method is probably ill suited to sodium caseinate.

6.2 Dextran and Pullulan

6.2.1 Materials: Dextran and Pullulan

Dextran T160 and pullulan were obtained from Pharmacia, (Uppsala, Sweden). All of the chemicals used were of analytical grade, obtained from either BDH Chemicals (BDH Ltd, Poole, England) or Sigma Chemical Co. (St Louis, MO), unless otherwise specified.

6.2.2 Sample Preparation: Dextran and Pullulan

All solutions were made in milliQ water containing (0.02% w/w) sodium azide, and filtered through a 0.025 μm Millipore filter. Two mere solutions of 10% w/w dextran in water and 10% w/w pullulan in water were stirred for two hours and left overnight at 5°C to ensure complete hydration. The two solutions were brought to room temperature the next day and filtered through a 0.22 μm Millipore. The dextran/pullulan mixtures were obtained by mixing the desired amount of dextran and pullulan solutions and filtered milliQ water.
The mixtures were left to equilibrate at 20°C the night before measurements were carried out.

Solutions of dextran (with a molecular mass of 160000 g/mol) and sodium azide in water, at concentrations of 1%, 2%, 4%, 6%, 8% and 10%, were investigated at a temperature of 25°C. Stock solution was made up at 10% w/w and then diluted to provide the lower concentration solutions. The solutions were stored at 5 degrees and used within two weeks of preparation to minimize the influence of bacterial growth.

Solutions of pullulan (with a molecular mass of 110000 g/mol) and sodium azide in water, at concentrations of 1%, 2%, 4%, 6%, 8% and 10%, were investigated at a temperature of 25°C. The solutions were prepared in the same way as the dextran solutions. Again,

solutions were stored at 5°C and used within two weeks of preparation to minimize the influence of bacterial growth.

Ternary solutions of dextran and pullulan in water were prepared by mixing suitable ratios of binary mixtures and diluting them to the concentrations required (1-10% in increments of 1% for the x = 1/4 and x = 3/4 solutions, and concentrations of 1%, 2%, 4%, 6%, 8% and 10% for x = 1/2).

The lowest concentration point in the experiments on dextran and pullulan was chosen to be the overlap concentration (c^*), as defined by the equation $2A_{2,11}M_{w1}c^* = 1$, where $A_{2,11}$ and M_{w1} are the second virial coefficient and the molecular weight of polymer 1 (dextran). It may be that the lowest concentrations used in this study belong in the dilute regime rather than the semi-dilute regime.

6.2.3 Experimental Methods: Dextran and Pullulan

The dynamic light scattering experimental setup used for the dextran/pullulan mixtures was changed from a pinhole collection method to a single mode fibre optic collection system, and a new photomultiplier was used, the signal from which was sent to the same autocorrelator used on the guar/dextran solutions.

The signal from the autocorrelator has been analyzed using three different methods. Both CONTIN and the newer version of the program CONTIN multiq, which allows the analysis of data from many angles simultaneously have been used, and, in addition, an analysis has also been carried out using the Kohlrausch-Williams-Watts (KWW) method. This method involves fitting the data to a sum of stretched exponentials using following equation

$$G_1 = A_1 \exp\left[\left(-\frac{t}{b_1}\right)^{B_1}\right] + A_2 \exp\left[\left(-\frac{t}{b_2}\right)^{B_2}\right] \quad + \quad + \qquad 6.2$$

The KWW approach attempts to accommodate the effects of polydispersity through the parameters b_i, which vary from zero to unity - small values are associated with broad distributions, while a value of 1 indicates a monodisperse solution. The mean relaxation times in the KWW method are given as

$$\langle t_i \rangle = \frac{b}{B_i} Gamma\left(\frac{1}{B_i}\right) \qquad 6.3$$

where gamma is the usual gamma function and B_i are the exponents in equation 6.2. CONTIN multiq has been described in chapter 4.6. The application of CONTIN multiq requires the setting of many parameters, and a comment on the effect using the dust term should be noted. If it was assumed that no dust term or one dust term for all angles was needed, then CONTIN multiq resolves the field autocorrelation function into two or three peaks of a diffusive nature and resolves no non-diffusive rates (two peaks at low concentrations, three at higher concentrations). If, however, a different dust term is assumed for different angles (which Provencher suggests is usually the best option), then a much better global fit is found and the signal is typically seen to consist of two non diffusive peaks and three narrow diffusive peaks (again, only two diffusive peaks at low concentrations). This is true for all the different compositions of solutions used.
A measure of the global fit (as outlined in section 4.6) is given in the output of CONTIN multiq in the form of SD(global). For the 10% concentration x = 1/2, solutions this value varies (with scattering angle) from 5.5×10^{-4} to 3.1×10^{-3} if one or no dust term is used, and from 4.1 - 5.6×10^{-4} if one is used for each angle.

Some data are presented to compare the results from the three analysis packages, some data analysed using CONTIN have been shown to illustrate the differences in results obtained at different scattering angles. The remaining data have been expressed in terms of the most recent and most reliable method viz CONTIN multiq. The data from all the binary and ternary solutions were passed through CONTIN using data from individual angles, through CONTIN multiq using all the angles at a given concentration as one data set, and though a KWW fit to the data at 90°.

The decay rates predicted by CONTIN were divided by q^2; converting them into apparent diffusion rates, the slope of the decay rates vs. q^2 is calculated to give a diffusion coefficient for each concentration.

Ioan, Aberle and Burchard[44] have carried out a comprehensive study on the properties of dextran in the semidilute concentration range in which they found that high concentration binary aqueous solutions of dextran exhibit two decay rates, one fast and one slow. From these decay rates, a fast diffusion coefficient and a slow diffusion coefficient were determined. Using a method combining static and dynamic light scattering they determined the self-diffusion coefficients of individual dextran molecules in solution. Unfortunately, there was no way to gather static light scattering data of sufficient precision available to the author of this work, so the approach taken by Ioan et al.[44] to establish the self-diffusion coefficients of the dextran molecules was not available.

Ioan et al.[44] describe the concentrations in terms of the universal parameter X (the fraction of total polymer concentration to the overlap concentration, X = c/c^* where $c^* = \frac{1}{M_W A_2}$).

In the dextran solutions used here X runs from 0.25 to 2.5.

A speculative approach is used by Ioan et al.[44] to determine the extent of association in dextran solutions. This is done by relating the measured apparent molecular weight at a given concentration (the reciprocal of the "osmotic modulus") to the molecular weight at infinite dilution. The approach is based on this well known equation from static light scattering

$$\frac{Kc}{R_{g=0}(c)} = \frac{1}{M_W}\left(1 + 2A_2 M_W c + 3A_3 M_W c^2 + \cdots\right) = \frac{1}{M_{app}(c)} \qquad 6.3$$

which they modify by replacing M_w (the molecular weight at infinite dilution) with $M_w(c)$ (the molecular weight at concentration c), indicating that the molecular weight of dextran changes with concentration - due to association in this case. By generating a plot of $M_w/M_{app}(c)$ against the reduced concentration X for three different molecular weights they

produced a master curve for the data. The master curve only fits well for the lower values of X. The deviation from this universal behaviour (master curve) is taken as evidence that the dextran molecules are associating to form clusters. By dividing the experimentally determined apparent molecular weight ($M_{app,\ exp}$(c)) by the apparent molecular weight predicted by the master curve (($M_{app,\ master}$(c)) they calculate the quantity $M_w(c)\ /M_w$ which is a measure of the true molecular weight of the dextran in solution at the concentration c, and so is an indication of the size of the clusters (see equation 23 ref. 3).

The deviation from universal behaviour occurs at lower values of X for lower molecular weights of dextran.

The dextran used in this study was of a molecular mass half that of the smallest they use and consequently the overlap concentration of the dextran binary solution used here was that much larger.

Such a low molecular mass dextran sample was chosen because there is evidence that at lower molecular weights the effects of branching are less pronounced[36] - therefore the theories based on a linear chain model could more reasonably be applied.

Interestingly, Ioan et al.[44] found that the self diffusion coefficients as calculated by their method coincided well with the slow diffusion coefficient, indicating that the motion of the individual molecules is dependent solely on the size of the larger associations, meaning that no molecule within the solution moves faster than the rate at which the larger associations move.

Though the value of X used here is fairly low, the small size of the molecules means that associative effects may be significant already. The slow decay rates observed here are probably due to the same mechanisms as in the solutions studied by Ioan et al.[44], but unfortunately the mechanisms are not understood. In fact Ioan et al.[44] end their paper with the statement "Our suggestions may be taken as an invitation to theoreticians to derive a well-founded theory based on measurable quantities".

6.2.4 Results: Dextran Binary Solutions

CONTIN multiq uses the most information to produce its results and is the most reliable method to extract information from the solutions, so the salient features produced by that method are previewed.

Two diffusive peaks are visible in dextran binary aqueous solutions at concentrations below 8%. At the highest two concentrations a third decay rate is detected with a small amplitude and a decay rate about one third that of the slow decay rate detected in the lower concentration solutions. CONTIN multiq also detects two non-diffusive decay rates (decay rates which do not vary with scattering angle), one at concentrations below 4% and two at concentrations of 4% and larger.
The prevailing theories on semidilute binary solutions are able to deal with one decay rate only, so even at the lower concentrations these are inadequate to describe binary dextran aqueous solutions.

The fast diffusion rate in the dextran solutions always contributes more than 0.9 of the signal attributed to diffusive sources. As the concentration of dextran increases, the slower decay rates contribute an increasing amount of the total signal attributed to diffusive sources.

The fast decay rates found with the CONTIN output applied to individual angles are plotted against q^2 (fig. 6.7). The resulting linear graphs clearly identify this decay rate as diffusive. The slope of the decay rates against q^2 gives a diffusion coefficient associated with a concentration. These fast diffusion coefficients are plotted against increasing concentrations (fig. 6.8), along with the fast diffusion coefficients produced by the CONTIN multiq and the KWW methods, in order to show the similarity between the different methods.

The fast diffusion coefficient is seen to increase steadily with increasing concentration. If the approach appropriate to dilute solutions is employed, then the data provide values of

$K_{D,2}$ = 10 ± 1 or 8.1 ± 0.5 g/cm^3 and $D_{z,0}$ = 3.3 ± 0.1 or 3.48 ± 0.08 10^{-11} m^2/s for the CONTIN multiq and KWW methods respectively.

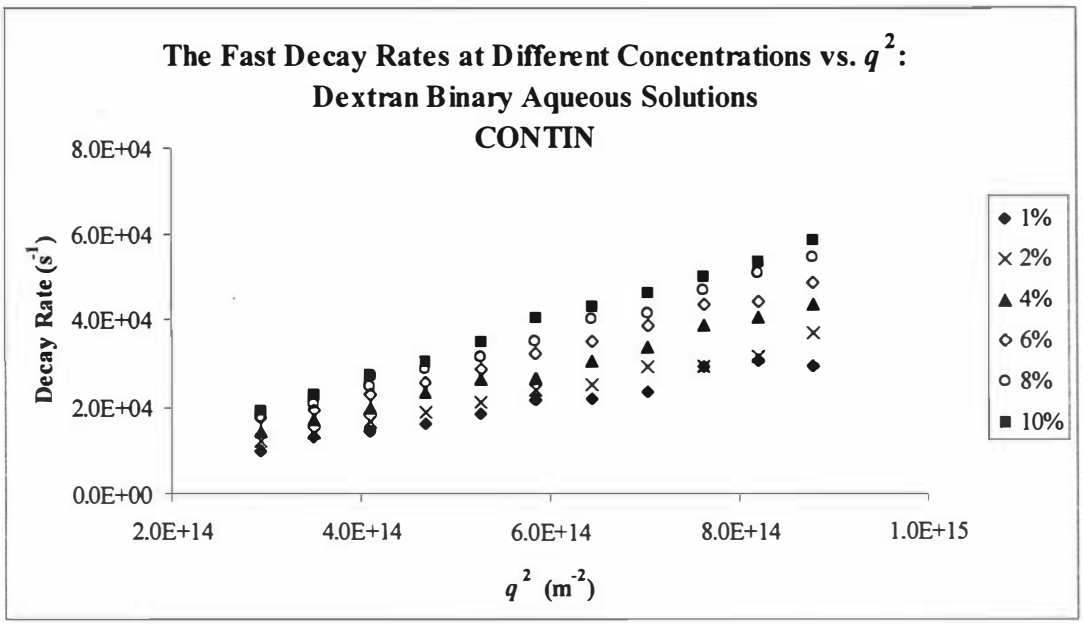

Figure 6.7 The fast decay rates measured on the different concentration dextran binary aqueous solutions plotted against q^2 the decay rates increase linearly with q^2 indicating the decay rates correspond to a diffusive mode in the dextran binary aqueous solutions

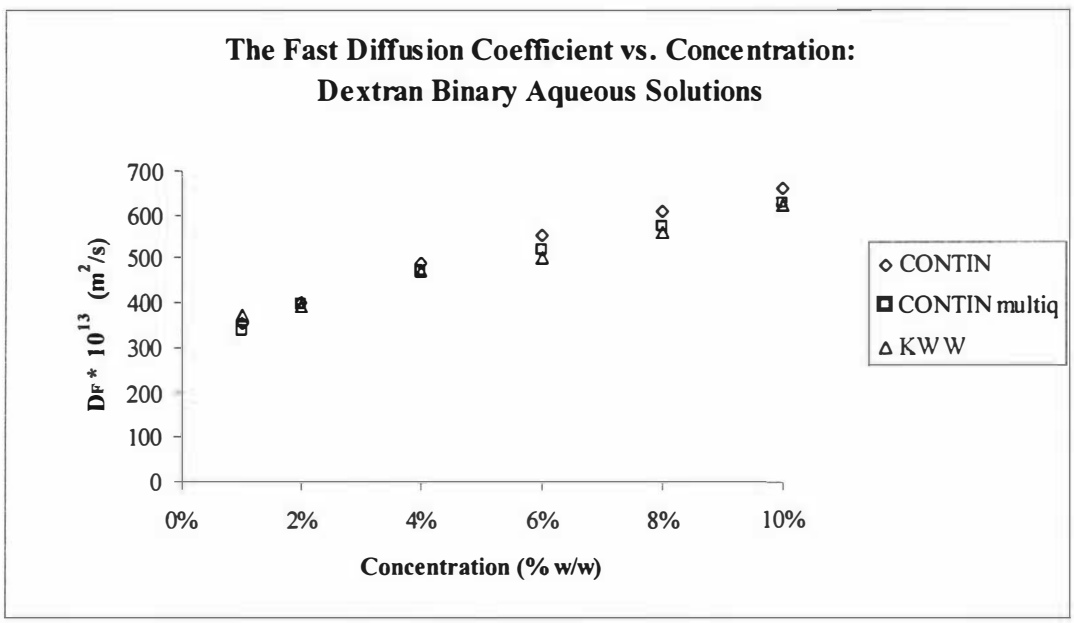

Figure 6.8 The fast diffusion coefficients obtained using the three different methods of analysis plotted against concentration for the dextran binary aqueous solutions

The slowest decay rate could scarcely be described as diffusive (linear with respect to q^2 with zero intercept) and does not appear in the CONTIN analysis for most angles in the low concentration data sets. The data show large scatter and are not well separated across the different concentrations (fig. 6.9).

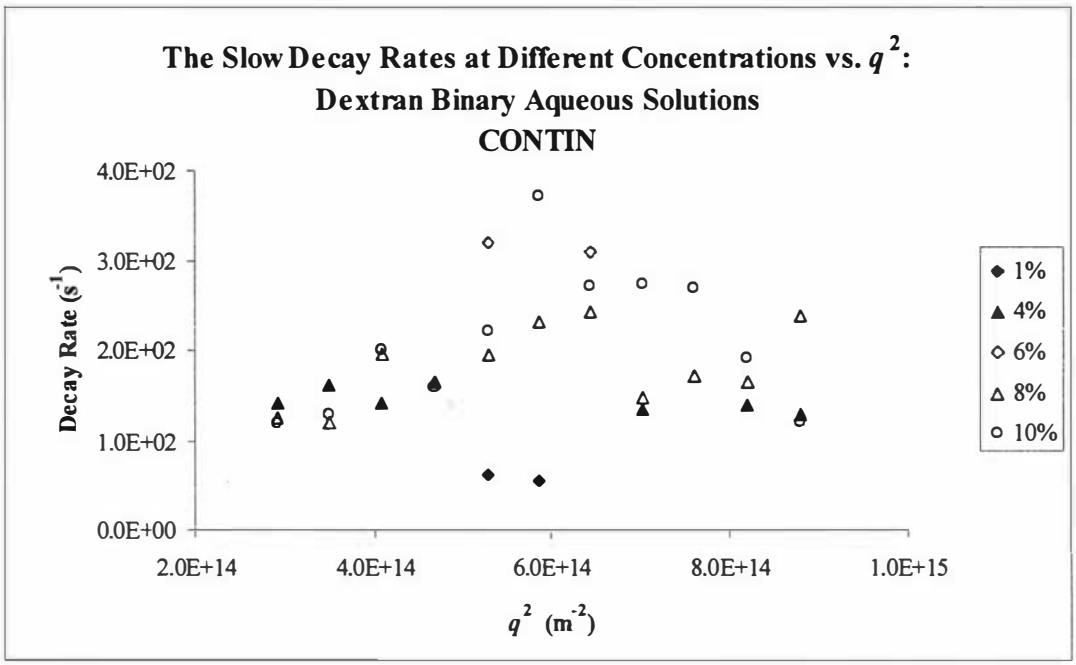

Figure 6.9 The slow decay rates measured in the dextran binary aqueous solutions plotted against q^2 the decay rates are not clearly diffusive, and few data are observed at low concentrations

CONTIN multiq only detected the slowest diffusion coefficient at the 8% and 10% concentrations. This diffusion rate appears with a relative amplitude of 0.07 and a diffusion coefficient of 6×10^{-13} m^2/s.

The CONTIN multiq analysis shows the mid diffusion coefficient at all concentrations. It has a value of approximately 3×10^{-12} m^2/s and shows no trend over concentration. The relative amplitude of this diffusion coefficient varies from 0.03 to 0.1, having the maximum value at 2% (fig. 6.10).

As mentioned above, CONTIN multiq also detects two non diffusive rates; one at 20 kHz, which appears across all concentrations, and one at 200Hz, which appears at concentrations

of 4% and above. Both these decay rates show a general increase with increasing concentration and both are around 0.05 the amplitude of the fastest diffusive rate at the highest concentration.

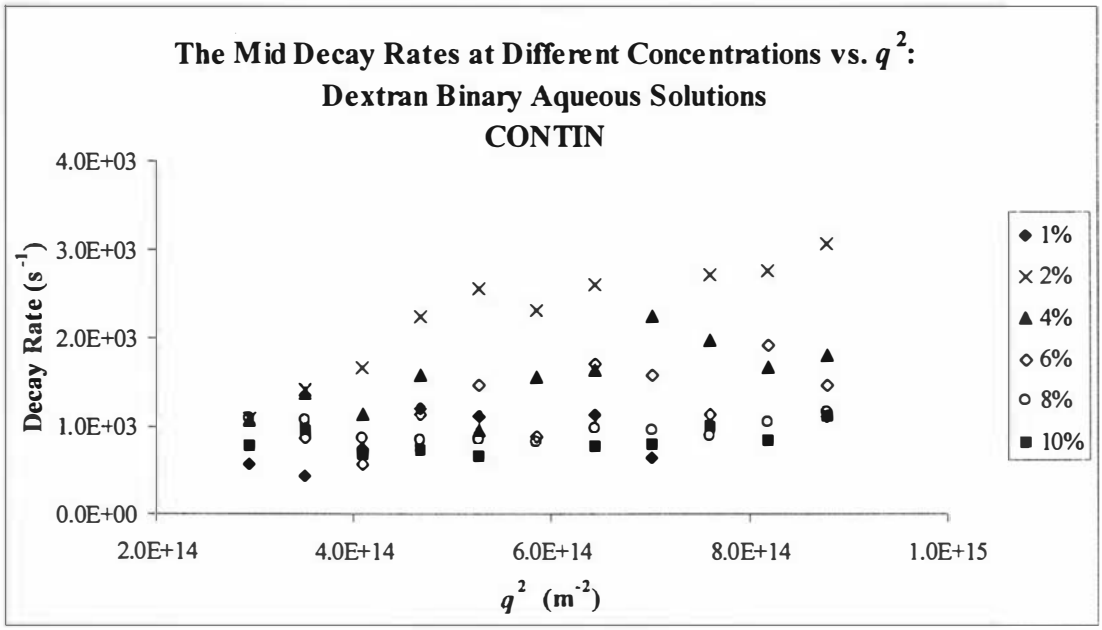

Figure 6.10 The mid decay rates measured in the dextran binary aqueous solutions plotted against q^2 the decay rates are not clearly diffusive

6.2.5 Discussion: Dextran

The slow diffusion coefficients for the dextran binary aqueous solutions are in the range of 10^{-13} m^2/s to 10^{-12} m^2/s. The cause of these slower diffusion coefficients in binary polymer solutions is poorly understood, the usual explanation being that they result from some kind of association between the polymers leading to large-scale correlations in the concentration fluctuations (see section 6.2.3). Such multiple modes have been observed before by Ioan et al.[44] and are attributed to the large scale clusters formed by groupings of the polysaccharides. If the polymers associate into larger particles and their translational motion is captured, then the measured decay rates would be expected to be diffusive in nature. Thus, CONTIN multiq supports the case that these diffusion coefficients detected are caused by the translational motion of groups of associated dextran molecules.

Wang provides a possible explanation for the non diffusive decay rates by considering the coupling of the concentration fluctuations to viscoelastic effects[45]. The framework provided by Wang predicts that the measured signal will consist of the usual diffusive rate plus a sum of q-independent rates which are related to the longitudinal stress modulus of the polymer network. The method outlined by Wang has a strong theoretical emphasis, and has not been couched in experimental terms.

6.2.6 Results: Pullulan

As with the dextran solutions, the CONTIN multiq analyses of the pullulan binary solutions yield very similar results to the other two analysis methods. Discussions of the other two methods are therefore limited to avoid repetition.

Two diffusion rates are visible to CONTIN multiq at concentrations of 2% and lower. At concentrations above 2% a third diffusion rate is detected with an amplitude about 1/10th that of the slow diffusion rate detected at low concentrations. This presents the same problems as with the dextran binary solutions.
CONTIN multiq also detects two non-diffusive rates; one appearing across all concentrations and one at concentrations of 6% and above.

As the concentration of pullulan increases the slower diffusive coefficients take up an increasing amount of the total signal attributed to diffusive sources. The proportion of these slower diffusion coefficients is larger in the pullulan binary solutions than in the dextran binary solutions, indicating that whatever causes these slower decay rates is more influential in the pullulan solutions than the dextran solutions.
The fastest diffusion coefficient is smaller in the pullulan solutions and increases more slowly with concentration than in the dextran binary solutions.

The relative amplitudes of all three diffusive decay rates detected in the pullulan system are nearly independent of q^2 - the slowest decay rates display a slight downward trend as q^2 increases, which is what would be expected from light scattering from large particles.

The relative amplitude of the slowest diffusion coefficient in the pullulan solutions is plotted vs. concentration in fig. 6.11. These data show that the relative amplitude increases from 0.1 at 4% to 0.2 at 10%.

Unlike the slowest decay rate in the dextran solutions, the case for the slowest decay rates in pullulan being diffusive is clearer - the slowest decay rate shows the same linear relationship to q^2 as the fast decay rate.

CONTIN multiq does not detect this diffusion process at the lowest two concentrations and shows a linear decrease from 1×10^{-12} m^2s^{-1} to 1×10^{-13} m^2s^{-1} over the higher 4 concentration points.

This slowest diffusion coefficient is presumed to be due to large scale associations in the pullulan networks.

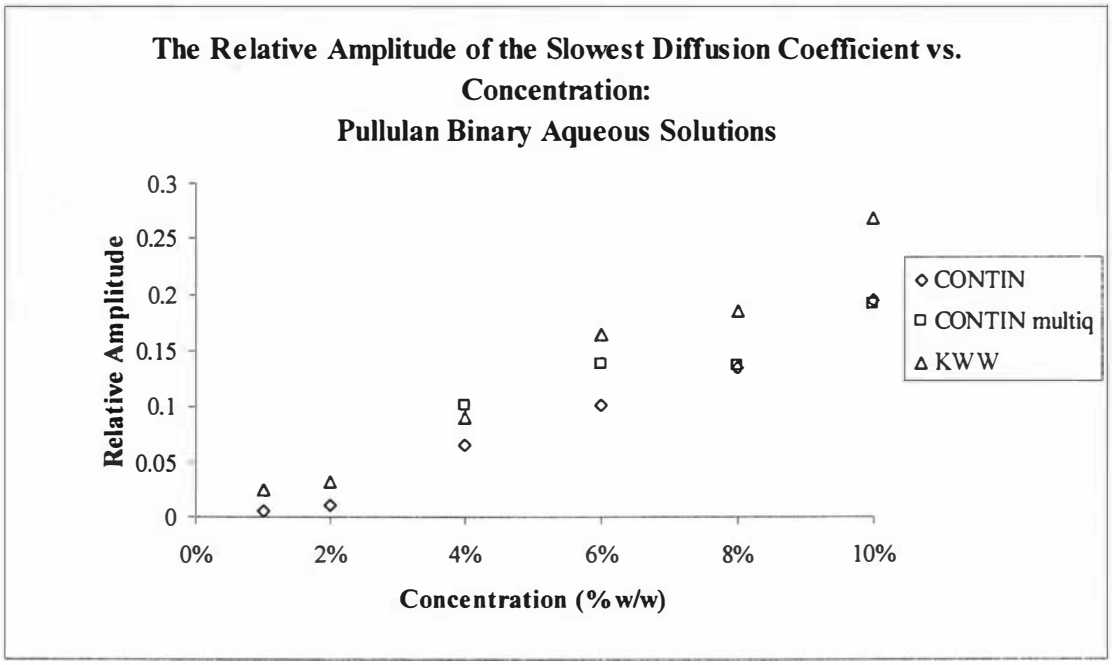

Figure 6.11 The relative amplitude of the slowest diffusion coefficient obtained using the three different methods of analysis for the dextran binary aqueous solutions plotted against concentration

The values of the fast diffusion coefficients in the pullulan solutions have been plotted against concentration (fig. 6.12). The fast diffusion coefficient increases steadily with increasing concentration from about 3.6×10^{-11} to 5×10^{-11} m^2s^{-1}. If, as with the dextran data, the approach applicable to dilute solutions is used, values of $K_{D,2} = 4.6 \pm 0.2$ or 4.1 ± 0.5 g/cm^3 and $D_{z,0} = 3.44 \pm 0.03 \times 10^{-11}$ or $3.37 \pm 0.08 \times 10^{-11}$ m^2/s are obtained for the CONTIN multiq and KWW methods respectively - the two different methods provide values which are consistent.

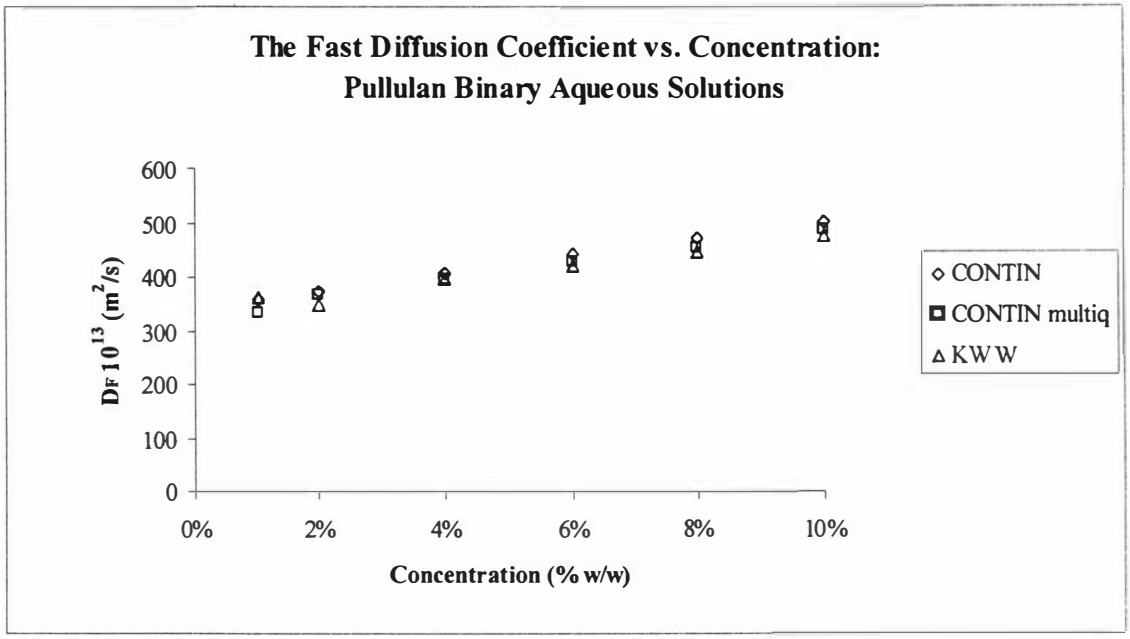

Figure 6.12 The fast diffusion coefficients obtained using the three different methods of analysis plotted against concentration for the pullulan binary aqueous solutions

The middle decay rates at the 1% and 10% concentrations in the pullulan system plotted against q^2 are shown in fig. 6.13. The data show that the mid decay rates have no clear dependence on q^2 at lowest concentration, while at the highest concentration there is a better correlation between decay rates and q^2. The diffusion coefficient is 1×10^{-12} m^2/s at 1% concentration, reaches a maximum value of 4.6×10^{-12} m^2/s at 6% concentration, then trends downward to 3.6×10^{-12} m^2/s at the 10% concentration.

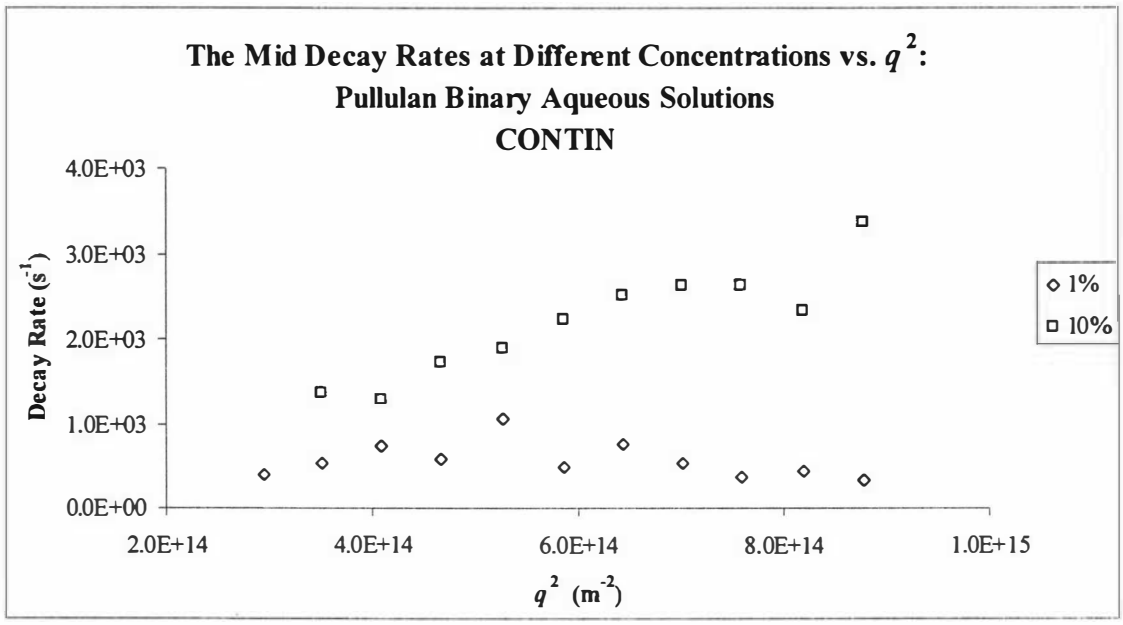

Figure 6.13 The mid decay rates measured at concentrations of 1% and 10% in the pullulan binary aqueous solutions plotted against q^2 the decay rates are not as obviously diffusive as the fast and slow decay rates at 1% concentration

The CONTIN multiq output of the relative amplitude of the middle diffusion coefficient present in the pullulan binary solutions (fig. 6.14) shows an increase at the lowest concentrations from 0.08 at 1% concentration to 0.1 at 2% concentration, followed by a decrease to 0.04 at the highest concentration.

These diffusion coefficients show trends very similar to those of the mid diffusion coefficients in the dextran binary solutions.

CONTIN multiq also detects non diffusive rates; one at 22 kHz which appears across all concentrations, and one at 200-150Hz which appears at concentrations of 6% and above. Both these relaxation rates show a general increase with increasing concentration. The amplitude of the slow relaxation rate divided by the amplitude of the fast diffusive rate increases from 0.07-0.12 as the concentration increases from 6% to 10%. The amplitude of the slow relaxation rate divided by the amplitude of the fast diffusive rate increases from 0.01 at the lowest concentration to 0.06 at the highest concentration.

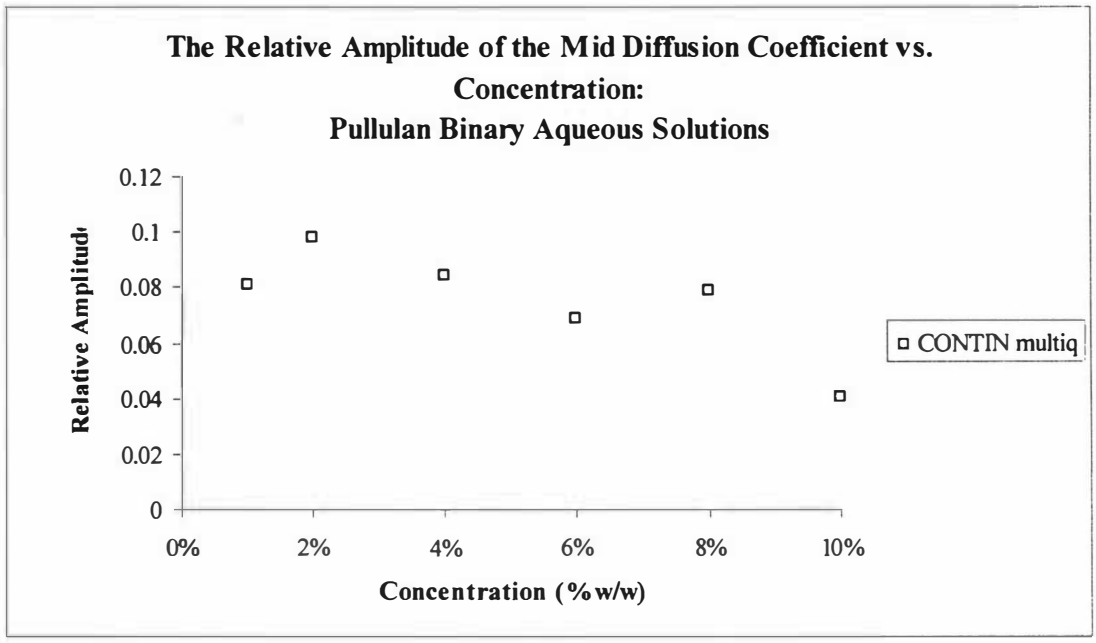

Figure 6.14 The relative amplitude of the mid diffusion coefficient obtained using CONTIN multiq for the pullulan binary solutions plotted against concentration

6.2.7 Ternary Solutions of Dextran and Pullulan

This section seeks to inform the reader of the main features determined by CONTIN multiq in the dextran/pullulan ternary solutions. As the results from the binary solutions are so qualitatively similar to the results expected from the ternary solutions, these features are also discussed in relation to the binary solutions. Once this is done, the $x = 1/4$ solutions are discussed in detail. The three different methods of analysis give results which have such similar trends, a table showing the relative values provided by the three methods is provided - otherwise only the results from CONTIN multiq are discussed for the sake of clarity. The results from CONTIN multiq on the $x = 1/2$ and $x = 3/4$ compositions are then discussed in relation to the $x = 1/4$ composition. The results of the application of the Sun and Wang theory are then discussed.

The most obvious feature of all these solutions is the diffusion process in the range from 3 $\times$ 10^{-11} to 6 $\times$ 10^{-11} m^2s^{-1} (the fast diffusion coefficient). This diffusion coefficient is consistently faster in the dextran binary solutions and decreases monotonically as the concentration of pullulan is increased. This diffusion coefficient increases as the total polymer concentration increases. Thus the fast diffusion coefficient increases with both composition and concentration.

The relative contribution of this fast diffusion coefficient to the sum of the amplitudes of the diffusive coefficients is greatest in the dextran binary solutions. The $x = 3/4$ solutions (mostly dextran) have the next largest fraction of signal from the fast diffusion coefficient. The symmetric composition ($x = 1/2$) typically has the lowest contribution from the fast diffusion coefficient and the pullulan and the $x = 1/4$ solutions usually having around the same fraction of fast to slow diffusion coefficient as the $x = 1/2$ solutions, albeit at marginally higher values.

There is also a mid diffusion coefficient which shows no clear trend as concentration increases, or as the composition changes - this coefficient is in the range of 2 $\times$ 10^{-12} to 8 $\times$

10^{-12} m^2 s^{-1}, and is a consistent feature present at all the different compositions and concentrations investigated.

The mid diffusion coefficient makes up the least amount of the measured signal, making up around 0.05 to 0.1 of the total signal from the diffusive processes. The relative amplitude of this diffusion coefficient shows no change as the total polymer concentration increases nor is there any clear trend to be seen as the composition changes.

A slower diffusion coefficient is also present at polymer concentrations of 4% and above - this slowest diffusion coefficient shows a consistent trend, decreasing from around 2×10^{-12} m^2s^{-1} to around 5×10^{-13} m^2s^{-1} as the concentration increases.

As previously stated, the slowest diffusion coefficient is not present in the most dilute binary solutions, in fact it is scarcely visibly in any solution with a total polymer concentration below 4%. The relative amplitude of this diffusion coefficient increases as the total polymer concentration increases, contributing around 0.1 of the signal at 4% total concentration to around 0.2 of the signal at the highest concentrations. The rate at which the relative amplitude of this diffusion coefficient increases is most pronounced for solutions which have more pullulan than dextran. The highest relative amplitude of this slowest diffusion rate is typically found in the $x = 1/2$ composition.

There are also peaks associated with relaxation rates. These peaks appear consistently in the higher concentration solutions at all compositions and have decay rates of about 200 Hz and 20 kHz. The amplitude of these rates is about 0.05 that of the fastest diffusion rate, and it is difficult to claim that there are any trends to these data points, although there does seem be a slight increase in the presence of the slower non-diffusive rates with increasing concentration. It is unlikely that these relaxation rates could have been determined without using CONTIN multiq as it would be very difficult to resolve relaxation rates on timescales so close to the diffusive decay rates.

While it seems clear that there are three diffusion processes present in all these solutions at high concentrations, the existence of the non diffusive rates is harder to corroborate given that they are not determined by CONTIN multiq if no or one baseline is assumed. However, given the difficulty in removing all possible sources of long term correlations and the much improved global fit when multiple baselines are used, it seems reasonable to assume that these non diffusive rates represent physical processes rather than an artefact of CONTIN multiq.

At the lower concentrations the slowest two diffusion coefficients are within a factor of 2 or 3 and so are hard to resolve, especially given the low relative amplitudes. It is perhaps unsurprising that clear trends in these diffusion coefficients and relative amplitudes are so hard to determine. However, the evidence for these three diffusion coefficients is good, as CONTIN multiq is designed to detect diffusive processes and provides a good global fit to the data.

The CONTIN fits to the data from each angle also support the case for three diffusive decay rates present in these solutions, although from these individual fits it is not as clear that the decay rates are diffusive.

6.2.8 Results: x=1/4

The trends of the x = 1/4 solutions with concentration are presented here, typically the three methods provide the same trends with concentration, but at a lower or higher value. A comparison of the results given by the different methods is given in table 6.3, the subscripts 1, 2, and 3 refer to slow, mid and fast diffusion coefficients respectively. The CONTIN value of each quantity has been used to normalize the CONTIN multiq and KWW value.

At concentrations above 4% the slow diffusion coefficient is seen to decrease with increasing concentration from 1.7 × 10^{-12} m^2/s to 5 × 10^{-13} m^2/s (fig. 6.15).

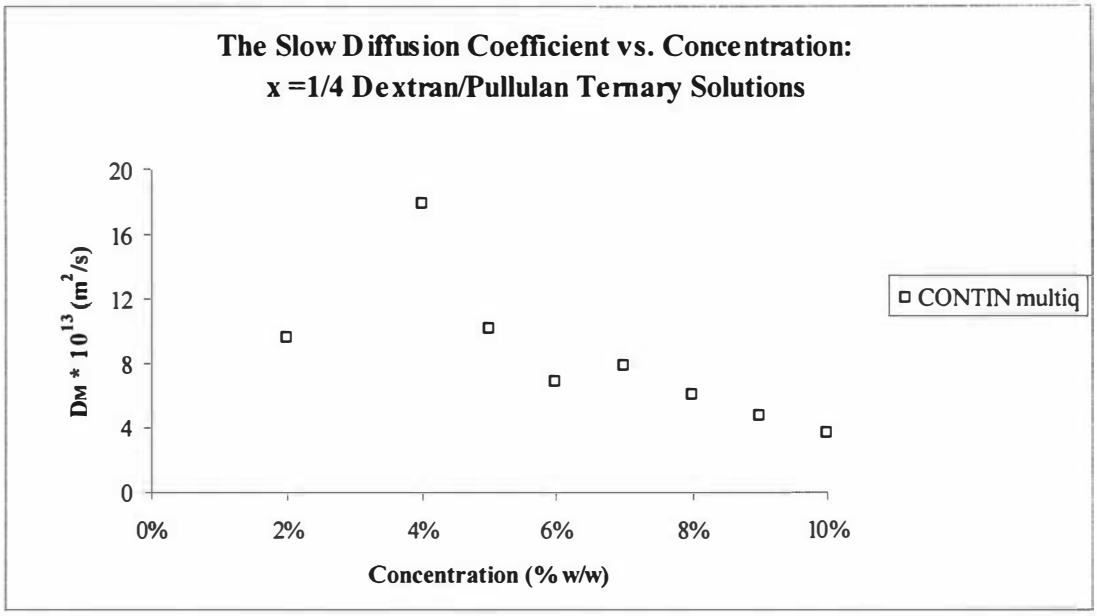

Figure 6.15 The slow diffusion coefficients obtained using CONTIN multiq plotted against concentration for the dextran/pullulan ternary solutions

The relative amplitudes of the three diffusion coefficients to the measured signal do not change appreciably with scattering angle, but do change with concentration. As the total polymer concentration increases, the relative amplitude of the slowest diffusion coefficient increases, from 0.02 of the signal at 2% total polymer concentration (C_T) to around 0.14 of the signal at C_T = 10% (fig. 6.16), as given by CONTIN multiq. This increase indicates

either an increase in the size of aggregates, or an increase in the number of aggregates. The three methods follow the same upward trend with concentration.

Table 6.3 A comparison of the different methods applied to the $x = 1/4$ solutions as values normalized against CONTIN.

	CONTIN multiq/CONTIN	KWW/CONTIN
$A_1/(A_1+A_2+A_3)$	1.05	1.66
$A_2/(A_1+A_2+A_3)$	1.15	1.66
$A_3/(A_1+A_2+A_3)$	0.98	0.9
D_1	1.55	0.85
D_2	1.34	1.45
D_3	0.96	0.89

The fast diffusion coefficient increases linearly with concentration from 3.8×10^{-11} m^2/s to 5.5×10^{-11} m^2/s.

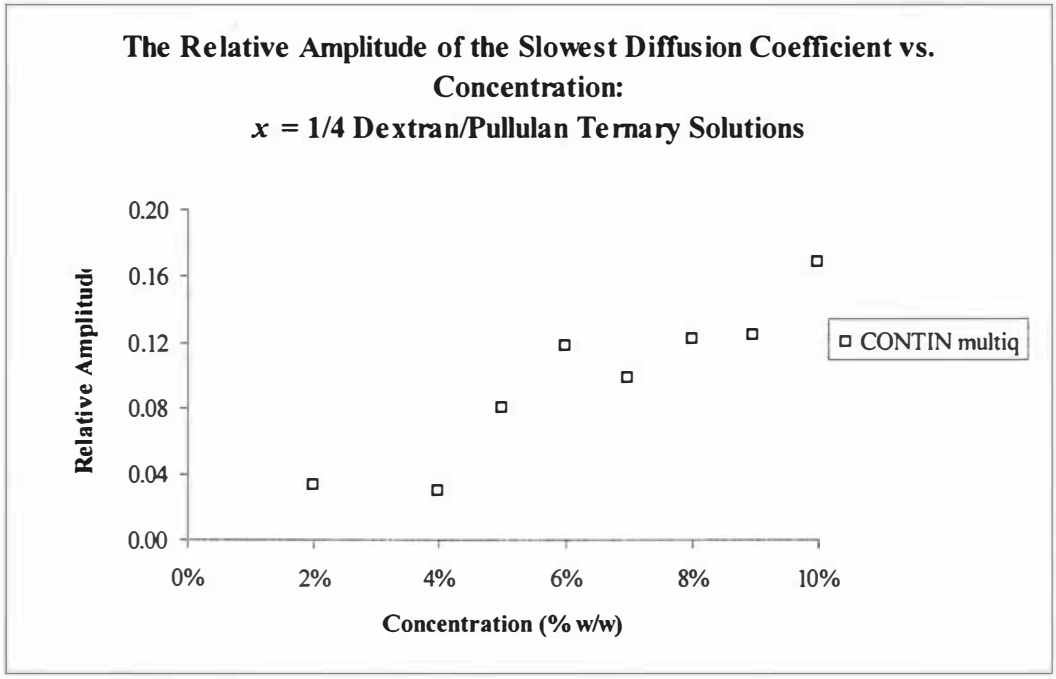

Figure 6.16 The relative amplitude of the slow diffusion coefficient obtained using the CONTIN multiq for the dextran/pullulan ternary solutions plotted against concentration - this mode shows an increase with concentration

The relative amplitude of this fast decay rate, as seen by CONTIN multiq, diminishes from 0.93 to 0.78 over the concentration range.

The mid diffusion coefficient increases from 2.4 × 10^{-12} m^2/s to 4.8 × 10^{-12} m^2/s over half the concentration range (1% - 5%) then decreases to 3.4 × 10^{-12} m^2/s as the concentration increases over 5% (fig. 6.17).

The relative amplitude of the mid decay rate, as given by CONTIN multiq, increases steadily over concentration from 0.05 to 0.08.

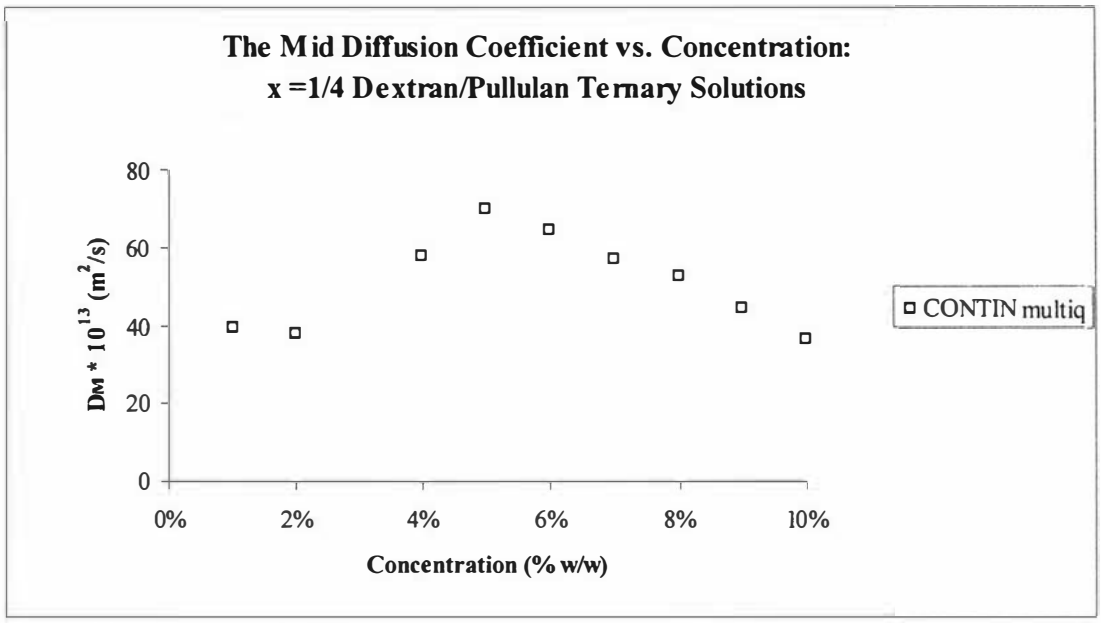

Figure 6.17 The mid diffusion coefficients obtained using CONTIN multiq plotted against concentration for the dextran/pullulan ternary solutions

6.2.9 Results: x=1/2 and x=3/4

Figures 6.18-21 show the comparisons between the three different composition values used. At a glance, it can be seen that the data show that there are no major differences between the different compositions.

Precise descriptions of these data sets would therefore be very similar, so, instead of detailing each composition independently, the differences between the different compositions are noted. These differences are in terms of the CONTIN multiq results. A summary of the relative values of the different quantities measured on the solutions are presented in table 6.4 in comparison to the x = 1/4 results.

The relative amplitude of the slowest diffusion coefficient (fig. 6.18) increases with concentration for all compositions studied. The relative amplitude is larger for the symmetric composition (x = 1/2) and is smallest for the x = 3/4 composition.

Table 6.4 A comparison of the values measured using CONTIN multiq averaged over concentration for different compositions, normalized against the x = 1/4 results.

	x=0	x=1/2	x=3/4	x=1
$A_1/(A_1+A_2+A_3)$	1.13	1.24	0.8	0.54
$A_2/(A_1+A_2+A_3)$	0.96	0.75	0.67	0.61
$A_3/(A_1+A_2+A_3)$	1.01	1.02	1.06	1.1
D_1	0.63	1.2	1.4	1.37
D_2	1.17	0.97	0.92	0.6
D_3	0.93	1.04	1.09	1.09

The relative amplitude of the slowest diffusion coefficient is lowest in the dextran binary solutions. Both the dextran and pullulan binary solutions show the slow diffusion coefficient at high concentrations. In general, the relative amplitude of this slowest diffusion coefficient is larger at low compositions. If this diffusion coefficient is related to

the aggregation or association of dextran or pullulan in solution then this would mean that as the relative amount of dextran is increased there is less aggregation.

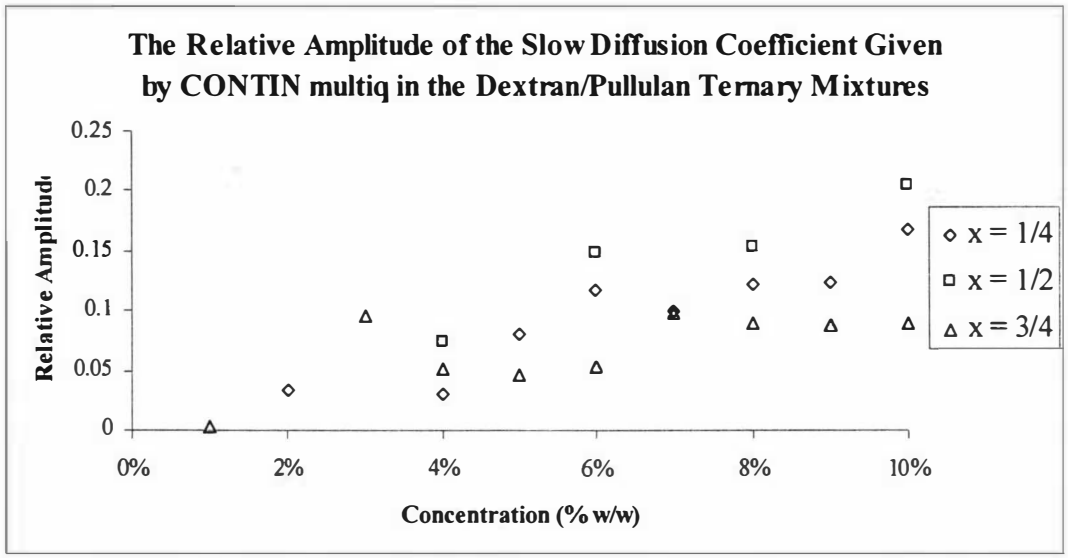

Figure 6.18 The relative amplitude of the slow diffusion coefficient at different compositions plotted against concentration in the dextran/pullulan ternary solutions

Fig. 6.19 shows the slowest diffusion coefficient for the three different compositions. The slowest diffusion coefficient decreases with increasing concentration for all compositions (all bar the lowest three concentration points). It is very difficult to discern trends across composition in this slowest diffusion coefficient.

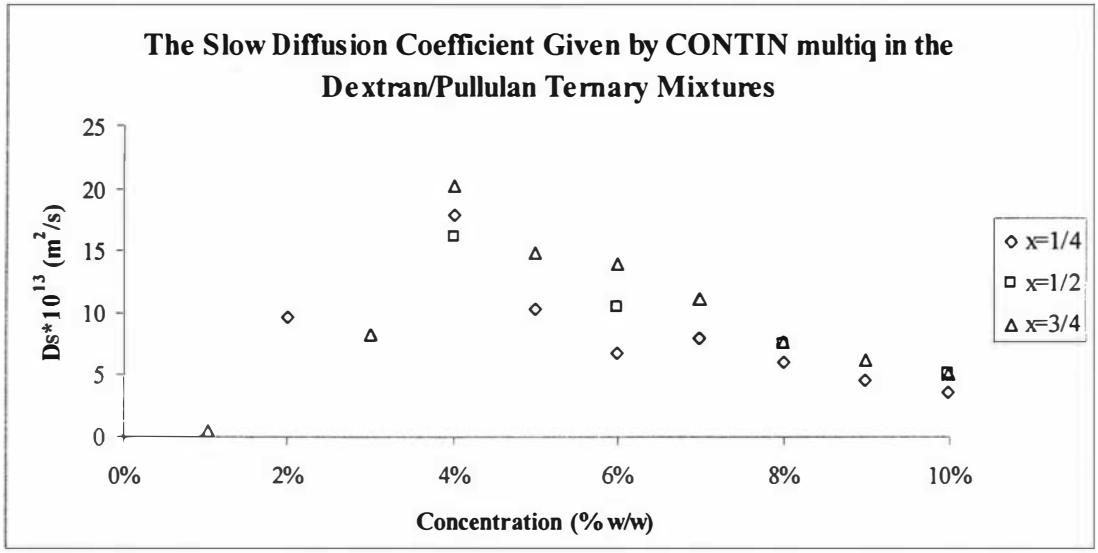

Figure 6.19 The slow diffusion coefficient at different compositions plotted against concentration in the dextran/pullulan ternary solutions

The relative amplitude of the mid diffusion coefficient does not show a trend across concentration for any but the x = 1/4 solutions, which shows an increasing relative amplitude over concentration. The mid diffusion coefficient typically rises and falls over the concentration range used (fig. 6.20). This diffusion coefficient is slowest in the dextran solutions and increases slightly in value as the composition decreases.

As with the slowest diffusion coefficient, trends in the relative amplitude of the mid diffusion coefficient are hard to discern. It does not increase or decrease with concentration. If the relative amplitude is averaged over concentrations 4% and higher then the results do show variation with composition. The dextran binary solutions show the lowest relative amplitude of the mid diffusion rate (0.05), with the relative amplitude increasing steadily to 0.09 at x = 1/4, before dropping to 0.07 in the pullulan binary solutions. The relative amplitude of the fastest diffusion coefficient decreases over concentration at all compositions used.

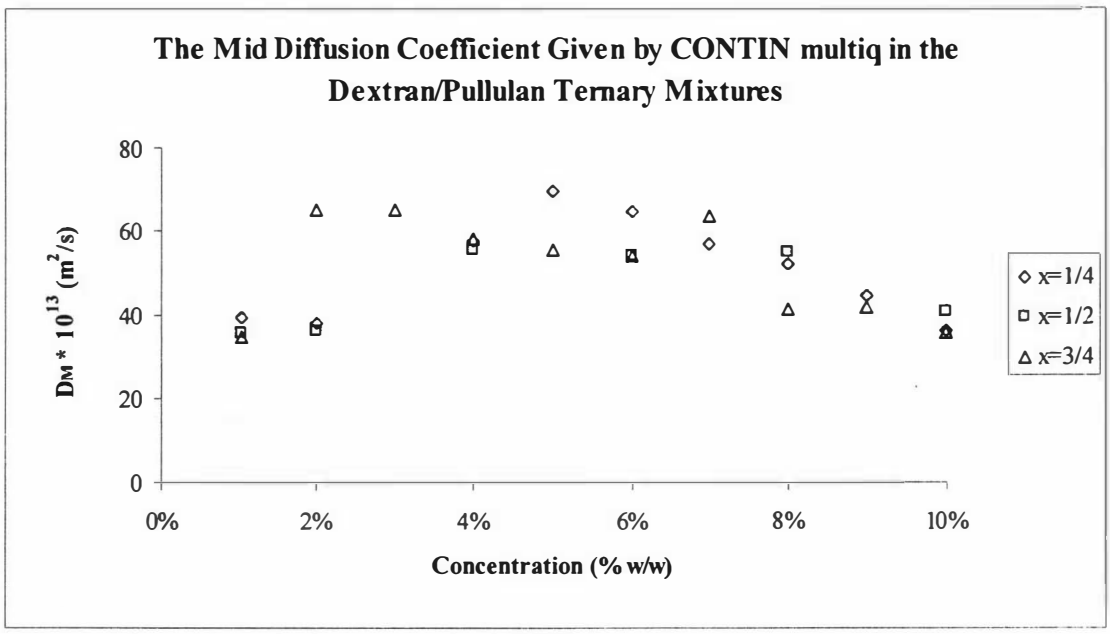

Figure 6.20 The mid diffusion coefficient at different compositions plotted against concentration in the dextran/pullulan ternary solutions

The fast diffusion coefficient data increases with concentration for all compositions and shows very little difference between compositions (fig. 6.21). This diffusion coefficient

increases slightly, but consistently, as the composition is increased. As the composition shifts towards dextran the fast diffusion coefficient increases.

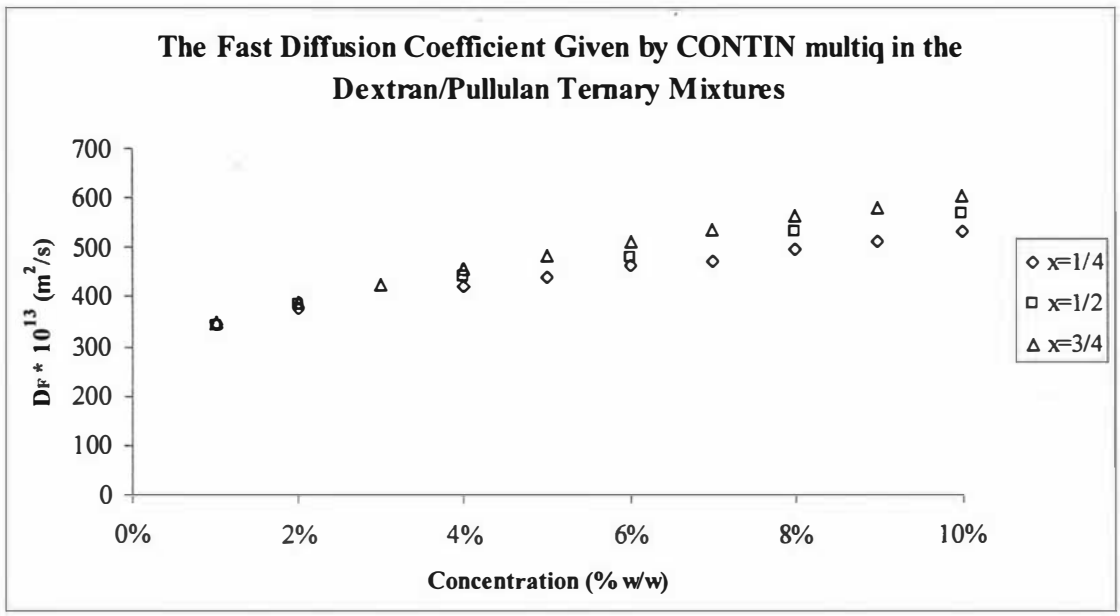

Figure 6.21 The fast diffusion coefficient at different compositions plotted against concentration in the dextran/pullulan ternary solutions

6.2.10 Application of the Sun and Wang Theory

The Sun and Wang theory requires that two diffusion coefficients are used to determine the self diffusion coefficients and cross virial coefficients - this poses a problem here, as there are three diffusion coefficients to choose from.

Somewhat arbitrarily, the fastest two modes are taken to be the eigenvalues of the system (see chapter 2). This choice is made simply because the slowest modes are judged to be most likely to be due to large scale associations.

The relative amplitude for use in the Sun and Wang theory is taken as the fraction of the mid diffusion rate to the sum of the amplitudes of the mid and fast diffusion rate. This relative amplitude trends upward as C_T increases.

The chosen two diffusion coefficients and relative amplitudes were entered into a program written with Mathematica to obtain solutions to the equations outlined by Sun and Wang.

This program has been tested using data from Sun and Wang's work[33] to ensure that results matching theirs were obtained.

The other two less likely combinations of slow and mid or slow and fast diffusion coefficients were also passed through the Mathematica program, but did not provide results any better than that of the mid and fast diffusion coefficients.

The calculated self-diffusion coefficients are expected to decrease with increasing concentrations - as the networks become denser the polymers move slower. This is true for D_{s2} but D_{s1} increases initially, and decreases only over the higher concentration range (fig. 6.22). It can be seen that the first three concentration points in this study have quite different characteristics, in particular figures 6.17 and 19 show a marked difference between these three points and the others. It may be that the theory is misapplied in the low concentration range and that the off diagonal elements of the mobility matrix are not negligible (see chapter 2). The Flory interaction parameter decreases with increasing concentration (fig. 6.23) - at the smallest concentrations χ_F is positive and is negative for the higher concentrations, which would imply a slight positive interaction force between the different polymer species.

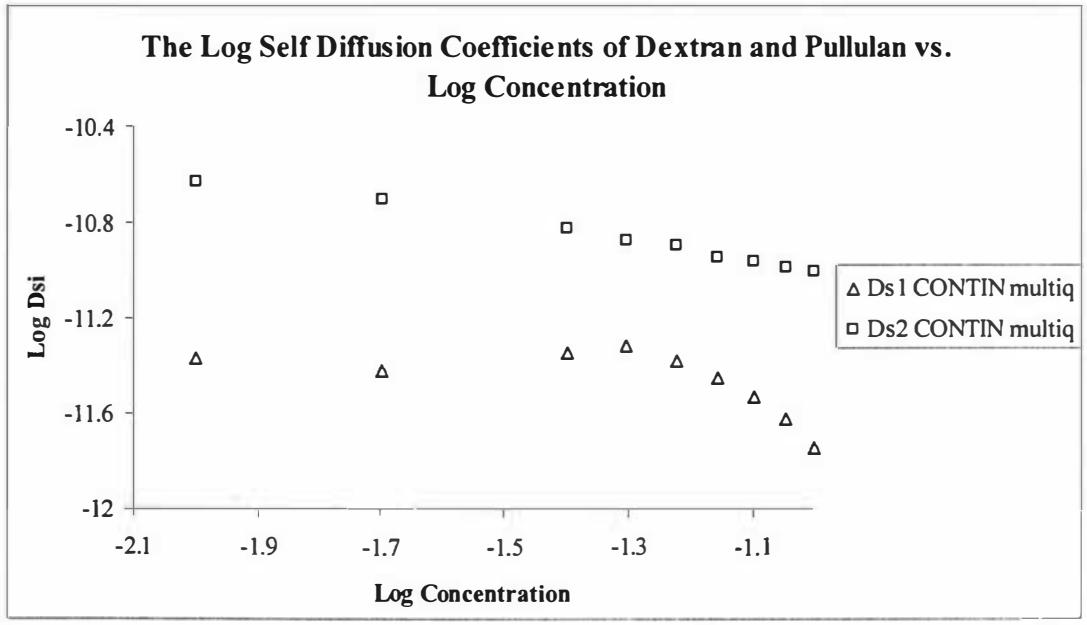

Figure 6.22 The self diffusion coefficients of dextran and pullulan in the dextran/pullulan ternary solutions obtained using the Sun and Wang theory

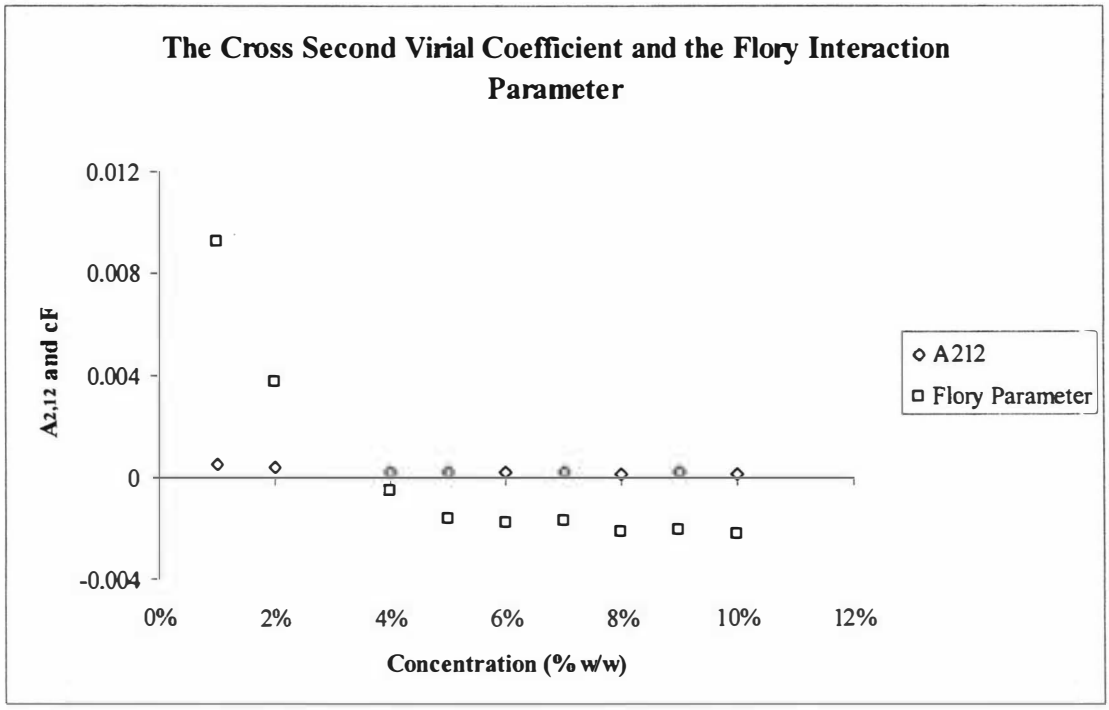

Figure 6.23 The cross second virial coefficient and the Flory interaction parameter in the x=1/4 dextran pullulan ternary solutions plotted against concentration

6.2.11 Discussion: Dextran and Pullulan Solutions

The aim of this work was to test the theory of Sun and Wang on non ideal ternary polymer systems; as such the data from the different compositions were put through a simple program written using Mathematica. While the x = 1/4 data produced results when such an approach was taken, no results could be obtained with the higher composition values. This was true no matter which two of the three diffusion coefficients were take to be the eigenvalues of the system.

With this in mind, one crude way of analyzing the data is just to say that the signal from the ternary solutions is simply the weighted sum of the signal from the binary solutions - for instance, that the x = 1/2 mixtures are simply the signals from one part dextran plus the signals from one part pullulan. If this approach is carried out, then the weighted average for the fast diffusion coefficients gives values smaller than the measured signals, meaning that

the interactions between the polysaccharides have shifted the rate towards the pullulan value. If these fast diffusion coefficients are taken as a measure of the interaction between the polymers, then the strength of the interactions governing concentration fluctuations are enhanced by the presence of pullulan.

It may be better to think of the two slowest diffusion rates as being due to the formation of clusters, as in semidilute polysaccharide solutions - perhaps due to the formation of clusters of differing sizes. In that case, it might be better to focus on the relative amplitude of the sum of slow modes to the sum of all diffusive modes to get an idea of the relative importance each process has at different concentrations. If the relative amplitudes are weighted by the fraction of dextran to pullulan and added together (i.e. at $x = 1/4$, three quarters the relative amplitude in pullulan is added to one quarter the relative amplitude in dextran) the results obtained consistently underestimate the relative amplitude of the slower diffusion rates. This indicates that the interactions between the unlike polysaccharides is increasing the signal due to large scale associations. The combined relative amplitude of the slow diffusion rates does not show much trend with composition - if anything it seems to increase at the mid composition rates, which would mean that the diffusion rates associated with the clusters have more influence at those compositions.

In addition to the diffusive modes, CONTIN multiq also detects the presence of two non-diffusive modes in solution. No quantitative explanation for these relaxation rates is attempted here, but the theory laid down by Wang[45] would be a good starting point.

The approach attempted here has proved difficult. The fact that the output from the binary solutions exhibits the same qualitative behaviour as the ternary solutions means that identifying the diffusion rates in the ternary systems as cooperative or interdiffusive modes is problematic, if not impossible. It may be stated clearly that the effects of polydispersity could make it more appropriate to think of these systems - both binary and ternary - as multicomponent polymer solutions (one component for each different polymer mass); such an approach is outside the scope of this work. However, having come so far, an effort was made to apply the usual theories to this unusual system. The fast diffusion rate is assumed

to be the cooperative mode (more correctly, the largest eigenmode of the diffusivity matrix) and the mid diffusion rate is taken to be the smaller eigenmode. The relative amplitude needed to use the Sun and Wang theory is taken as the relative amplitude of the mid diffusion rate to the sum of the amplitudes of the mid and fastest diffusion rate (the slow diffusion rate is ignored). By using this method, values for D_{s1}, D_{s2} and $A_{2,12}$ can be obtained for the $x = 1/4$ solutions and the higher concentrations of the $x = 1/2$ solutions - no mathematical solutions could be found for the $x = 3/4$ solutions.

When this is done, the self diffusion rate of dextran $x = 1/4$ is found to decrease from 2×10^{-12} m^2s^{-1} to 3×10^{-13} m^2s^{-1} over the concentration range studied. At $x = 1/2$, slightly larger values were found. The self diffusion rate of pullulan decreases from 1.6×10^{-11} m^2s^{-1} to 1×10^{-11} m^2s^{-1} over the concentration range. At $x = 1/2$, the self diffusion rates are about 50% higher. The dextran molecule is 45% more massive than pullulan but this alone would not explain such a large discrepancy between the two self diffusion coefficients.

The Flory interaction parameter decreases with increasing concentration, at the smallest concentrations χ_F is positive and is negative for the higher concentrations, which would imply that the interaction force between the different polymer species changed from a repulsive force to an attractive force as the concentration increased.

6.2.12 Conclusion: Dextran and Pullulan Solutions

In summary, the dynamics of semidilute polysaccharides are complex. The lack of a coherent theory to explain these dynamics when more than one mode is present in solutions means that the data are very difficult to interpret.

The ternary solutions show distressingly little difference from the binary solutions, this is surprising because the interactions between unlike polymers are expected to manifest as an additional peak. The qualitative similarity between the results for different solutions lends to the conclusion that the interactions between the monomers of unlike polysaccharides

used here are very similar in their nature to the interactions between the monomers of like polysaccharides.

The CONTIN and CONTIN multiq results provide values of the fast diffusion coefficients which are within 5% of each other, the two slower diffusion coefficients are out by around 50%. The relative amplitudes of the three diffusion coefficients given by these two methods are within 15%. The errors in the amplitudes and diffusion coefficients given by CONTIN at one angle are larger than those given by CONTIN multiq using all angles at once. When the results from each angle analysed using CONTIN are taken together, the errors from CONTIN and CONTIN multiq are seen to be within a few percent of each other. However, only by using CONTIN at differing angles can the assumptions which CONTIN multiq uses be tested, for instance that the amplitudes are independent of scattering angle. The CONTIN multiq method is the only way of determining the relaxation modes present in solution. The KWW method provides results which are similar to those of CONTIN and CONTIN multiq, but there is much more scatter over the concentration range used showing that this method does not provide such reliable results as the other two.

The presence of two slow diffusive rates in addition to the fast diffusion rate is taken to indicate the formation of large scale associations or clusters in the semidilute solutions. These modes may be masking the expected "interdiffusive mode" in the ternary solutions. These diffusion rates are larger in the mixtures than would be expected given the presence of dextran or pullulan individually, indicating that the combination of these molecules increases the formation of clusters.

Future work in this area might choose to attempt to explain the presence of the relaxation rates in terms of viscoelastic coupling effects.

The ability to gather data on semidilute polysaccharide solutions has increased beyond the capacity of theory to explain it. Hopefully this work will help spur theoretical effort to explain the dynamical properties of polysaccharide solutions.

7

Summary and Future Work

The DLS study of polysaccharides at semi dilute concentrations has proved a difficult task. All three biopolymer systems investigated here have shown behaviour which is consistent in form with the theoretical framework used to investigate ternary polymer solutions - however, the presence of long scale correlations, which do not as yet have a firm theoretical explanation has proved impossible to explain.

The technique of dynamic light scattering is quick and reveals information about the fluctuations in solution; however, the ill-posed nature of resolving the measured intensity autocorrelation function into a sum of decaying exponentials means that small errors in the measured function can lead to unbounded errors in the resolved decay rates.
To this end a modified version of CONTIN (CONTIN multiq) has been used to analyze the data from the dextran/pullulan mixtures. CONTIN multiq takes the data from all angles measured on one sample and makes the assumption that there is one process behind the light scattered at different angles. By fitting the data at different angles to one model there is much more information available to resolve the decay rates in the intensity autocorrelation signal. In its default setting CONTIN multiq provides an output which has two grids, one for diffusive decay rates, and one for non diffusive decay rates. When CONTIN alone was used on the dextran/pullulan system it was impossible to resolve the non diffusive peaks resolved when CONTIN multiq was used.

However, the assumptions which CONTIN multiq uses can only be tested by using CONTIN at differing angles. The CONTIN multiq method is the only way of determining the relaxation modes present in solution. The KWW method provides results which are similar to those of CONTIN and CONTIN multiq - there is no advantage to using this technique in preference to CONTIN multiq.

One major concern here must be that the solutions used have not been left for long enough to equilibrate. All the solutions were measured within one week of preparation. This was done to minimize the effects of microbial action and also because of the known tendency of polysaccharides to form aggregates in solution which would adversely affect the experimental results. It is possible that the solutions were still coming to equilibrium when measured.

There is much work to be done on the study of the thermodynamics of biopolymer solutions, and this thesis has aimed to determine whether the method outlined by Sun and Wang can be applied to biopolymer solutions.

Of the parameters measured by this method, the self diffusion coefficients and the Flory interaction parameter, the self diffusion coefficients are hardest to determine using other methods - the parameter most amenable to comparison with other work is the Flory interaction parameter, which can be determined by tie line analysis.

Given the failure to match the Flory interaction parameter determined here with that of the results given in the literature, this work suggests that the Sun and Wang method must be considered inadequate for the systems at hand.

7.1 Future Work

The work done suggests that the interpretation of dynamic light scattering data requires considerably more investment in theoretical techniques. The presence of long term correlations present even in the binary solutions studied are typically explained in terms of aggregates formed from the biopolymers. The process of formation of these aggregates is not clear.

Developing theories which explain the formation of aggregates (assuming they were causing the long term correlations) and how they modify the interactions between unlike polymers and their translational diffusion coefficients would be an interesting avenue for future research.

The emphasis in this work was to take commercial grade biopolymers soluble in water for investigation, as these are widely available and their properties are of most interest to the food industry. These biopolymers typically have a higher polydispersity than synthetic polymers and no effort was made to fractionate the samples used here.

Future work may look at samples of biopolymers which have been fractionated to achieve results more specific to homopolymers.

In conjunction with tie-line analysis, other ternary polymer systems could be investigated with the aim of finding a systematic relationship between the Flory interaction parameter found using tie line analysis and that found using dynamic light scattering.

Bibliography

1 Burchard, W. In Harding, S. E., Sattelle, D. B., Bloomfield, V. A. (Eds) *Static and Dynamic Light Scattering Approaches to Structure Determination of Biopolymers* (Royal Society of Chemistry, Cambridge, 1992).

2 Akcasu, A. Z. *Dynamic Scattering from Multicomponent Polymer Mixtures in Solution and in Bulk* In Brown, W. (Ed.) *Dynamic Light Scattering, The Method and Some Applications* (Oxford, UK, 1993).

3 Akcasu, A. Z. *Macromolecular Theory and Simulations* **6**, 679-702 (1997).

4 Akcasu, A. Z., Nagele, G. & Klein, R. *Macromolecules* **24**, 4408-4422 (1991).

5 Benmouna, M., Benoit, H., Duval, M. & Akcasu, Z. *Macromolecules*, **20**, 1107-1112 (1987).

6 Foley, G. & Cohen, C. *Macromolecules* **20**, 1891 (1987).

7 Genz, U. *Macromolecules* **27**, 3501-3512 (1994).

8 Genz, U. *Macromolecules* **27**, 5691-5696 (1994).

9 Hammouda, B. *Macromolecules* **26**, 4800-4804 (1993)

10 Pinder, D. N. *Trends in Macromolecular Research* **1**, (1994).

11 Sun, Z. & Wang, C. H. *J. Chem. Phys.* **103**, 3762-3766 (1995).

12 Wang, C. H. *J. Chem. Phys.* **107**, 3675-3683 (1997).

13 Aven, M. R. & Cohen, C. *Macromolecules* **23**, 476-486 (1990).

14 Borsali, R., Duval, M., Benoit, H. & Benmouna, M. *Macromolecules*, **20**, 1112-1115 (1987).

15 Borsali, R., Duval, M. & Benmouna, M. *Macromolecules*, **22**, 816-821 (1989).

16 Brown, W. & Rymden, R. *Macromolecules* **21**, 840-846 (1988).

17 Brown, W. & Zhou, P. *Macromolecules* **22**, 4031-4039 (1989).

18 Brown, W. & Zhou, P. *Macromolecules* **23**, 5097-5101 (1990).

19 Daivis, P.J., Pinder, D.N. & Callaghan, P. T. *Macromolecules* **25**, 170-178 (1992).

20 Daivis, P.J., Pinder, D.N. & Callaghan, P. T. *Macromolecules* **26**, 3381-3390 (1993).

21 Fukuda, T., Nagata, M. & Inagaki, H. *Macromolecules* **19**, 1411-1416 (1986).

22 Geible, L., Benmouna, M., Borsali, R. & Fischer, E. W. *Macromolecules* **26**, 2433-2438 (1993).

23 Giebel, L., Borsali, R., Fisher, E. W. & Benmouna, M. *Macromolecules*, **25**, 4378-4381 (1992).

24 Giebel, L., Borsali, R., Fisher, E. W. & Meier, M. *Macromolecules* **23**, 4054-4060 (1990).

25 Kent, M. S., Tirrell, M. & Lodge, T. P. *Macromolecules*, **25**, 5383-5397 (1992).

26 Pinder, D. N. *Macromolecules* **30**, 226-235 (1997)

27 Sasaki, K. & Hashimoto, T. *Macromolecules* **17**, 2818-2825 (1984).

28 Seils, J., Benmouna, M., Patkowski, A. & Fischer, E. W. *Macromolecules*, **27**, 5043-5051 (1994).

29 Straziell, C., Duval, M. & Benmouna, M. *Macromolecules* **27**, 4960-4967 (1994).

30 Su, A. C. & Fried, J. R. *Macromolecules* **19**, 1417-1421 (1986).

31 Sun, Z. & Wang, C. H. *J.Chem. Phys.* **112**, 6844-6850 (2000).

32 Sun, Z. & Wang, C. H. *Macromolecules* **30**, 4939-4944 (1997).

33 Sun, Z. & Wang, C. H. *Macromolecules* **29**, 2011-2018 (1996).

34 Desbrieres, J., Borsali, R., Rinaudo, M. & Milas, M. *Macromolecules* **26**, 2592-2596 (1993).

35 Simonet, F., Garnier C. & Doublier, J.-L. *Carbohydrate Polymers*, **47**, 313-321 (2002).

36 Nordmeier, E. *Journal of Physical Chemistry* **97**, 5770-5785 (1993).

37 Vilgis, T. A., Benmouna, M. & Benoit, H. *Macromolecules*, *24*, 4481 (1991).

38 Doi, M. & Edwards, S. F. *The Theory of Polymer Dynamics* (Oxford University press, Belfast, 1986).

39 Benmouna, M., Seils, J., Meier, G., Pakowski, A. & Fisher, E. W. *Macromolecules*, **26**, 668-678 (1993).

40 Hess, W. In Degiogio, V., Corti, M., Giglio, M. (Eds.) *Light Scattering in Liquids and Macromolecular Solutions* (Plenum Press, New York, 1980).

41 Dhont J. K. G. *An Introduction to Dynamics of Colloids* (Elsevier, Amsterdam, 1996).

42 Ackasu, A. Z. *Macromolecules* **22**, 3682 (1989).

43 Lal, J. & Bansil, R. *Macromolecules* **24**, 290 (1991).

44 Ioan, C. E., Aberle T. & Burchard, W. *Macromolecules* **34**, 326-336 (2001).

45 Wang, C. H. *Macromolecules* **25**, 1524-1529 (1992).

46 Hsu, C. C. & Prausnitz, J. M. *Macromolecules* **7**, 320 (1974).

47 Koningsveld, R. & Kleintjens, L. A. *Macromolecules* **4**, 637 (1971).

48 Koningsveld, R. & Stockmayer, W. H. *Macromolecules* **7**, 73 (1974).

49 Solc, K. *Macromolecules* **19**, 1166 (1986).

50 Kamide, K. *Thermodynamics of Polymer Solutions: Phase Equilibria and Critical Phenomena* (Elsevier, Amsterdam, 1990).

51 Kurata, M. *Thermodynamics of Polymer Solutions.* (Harwood Academic Publishers, USA, 1982).

52 Fujita H. *Polymer Solutions.* (Elsevier, Amsterdam, 1990).

53 Solc, K. (Ed.) *Polymer Compatibility and Incompatibility: Principles and Practices* (Harwood Academic Publishers, Cooper Station, N.Y., 1982, vol 2 in MMl Press Symposium Series), p1-24.

54 Sariban, A. & Binder, K. *Macromolecules* **21**, 711 (1988).

55 Tompa, H. *Polymer Solutions* (Butterworths, London, 1956), p183.

56 Zeman, L. & Patterson, D. *Macromolecules* **5**, 513 (1972).

57 Solc, K. & Koningsveld, R. *J.Chem.Phys.* **89**, 2237 (1990).

58 Stick, R. V. *Carbohydrates:The Sweet Molecules of Life* (Academic Press, 2001).

59 Gamini, A. & Mandel, M. *Biopolymers*, **34**, 783-797 (1994).

60 Sato, T., Norisuye, T & Fujita, H. *Macromolecules* **17**, 2696-2700 (1984).

61 Capron, I., Brigand, G. & Muller, G. *Polymer* **38**, 5289-5295 (1997).

62 Capron, I., Brigand, G. & Muller, G. *International Journal of Biological Macromolecules* **23**, 215-225 (1998).

63 Hacche, L. S., Washington, G. E. & Brant, D. A. *Macromolecules* **20**, 2179-2187 (1987).

64 Pouliout, Y., Gauthier, D. F. & Bard, C. *J. Food Sci. 60*, 111-116 (1995).

65 Lynch, A. G., Mulvihill, D. N., Law, A. J. R., Leaver, J. & Horne, D. S. *Int. Dairy Journal* 7, 213 –220 (1997).

66 Ioan, C. E., Aberle T. & Burchard, W. *Macromolecules* **33**, 5730-5739 (2000).

67 Ioan, C. E., Aberle T. & Burchard, W. *Macromolecules* **34**, 3765-3771 (2001).

68 Aspinall, G. O. *Polysaccharides* (Academic Press, 1983) p477.

69 Richardson, P. H., Clark, A. H., Russell, A. L., Aymard, P. & Norton, I. T. *Macromolecules* **32**, 1519-1527 (1999).

70 Gittings, M. R., Cipelletti, L., Trappe, V., Weitz, D. A., In, M. & Marques, C. *Journal of Physical Chemistry B*. **104**, 4381-4386 (2000).

71 Gittings, M. R., Cipelletti, L., Trappe, V., & Weitz, D. A., In, M. & Lal, J. *Journal of Physical Chemistry A*. **105**, 9310-9315 (2001).

72 Chu, B. *Laser Light Scattering* (Academic Press, New York, 1974).

73 Berne, B. J. & Pecora, R. *Dynamic Light Scattering* (John Wiley and Sons, New York, 1976).

74 Crosignani, B., Porto, P. D. & Bertolotti, M. *Statistical Properties of Scattered Light* (Academic Press, New York, 1975).

75 Cummings, H. Z. & Pike, E. R. *Photon Correlation and Light Beating Spectroscopy* (Plenum Press, New York, 1974).

76 Brown, W. (Ed.) *Dynamic Light Scattering, The Method and Some Applications.* (Clarendon, Oxford University Press, 1993).

77 Provencher, S. W. *Computer Physics Communications* **27**, 213-227 (1982).

78 Provencher, S. W. *Computer Physics Communications* **27**, 229-242 (1982).

79 Stepanek, P. & Provencher, S. W. *Macromolecular Symposium* **162**, 191-203 (2000).

80 Buttgereit, R., Roths, T., Honerkamp, J. & Aberle, L. B. *Physical Review E* **64**, 041401-1-10 (2001).

81 Pinder, D. N., Nash, W., Hemar, Y. & Singh, H. *Food Hydrocolloids* **17**, 463-468 (2003).

82 Yi, L. Ph. D, Massey, 1996.

83 Ricka, J. *Applied Optics* **32**, 2860-2874 (1993).

84 Gisler, T., Ruger, H., Egelhaaf, S. U., Tschumi, J., Schurtenberger, P. & Ricka, J. *Applied Optics* **34**, 3546-3553 (1995).

85 Capron, I., Alexandria, S. & Muller, G. *Polymer*, *39*, 5725-5730 (1998).

86 Dickenson, E., Semenova, G. & Antinpova, A. S. *Food Hydrocolloids* **12,** 227-235 (1998).

87 Milas, M., Reed, W. F. & Printz, S. *International Journal of Biological Macromolecules* **28**, 211-221 (1996).

88 Rodd, A. B., Dunstan, D. E. & Boger, D. V. *Carbohydrate Polymers* **42**, 159-174 (2000).

89 Coviello, T., Kajiwara, K., Burchard, W., Dentini, M. & Crescenzi, V. *Macromolecules* **19**, 2826-2831 (1986).

90 Coviello, T., Burchard, W., Dentini, M. & Crescenzi, V. *Macromolecules* **20**, 1102-1107, (1987).

91 Southwick, J. G, Jamieson, A. M., Blackwell. J. *Macromolecules* **14**, 1728-1732 (1981).

92 Paradossi, G. & Brant, D. A. *Macromolecules* **15**, 874-879 (1982).

93 Milas, M., Rinaudo, M., Duplessix, R., Borsali, R. & Lindner, P. *Macromolecules* **28**, 3119-3124 (1995).

94 Tinland, B. & Rinaudo, M. *Macromolecules* **22**, 1102-1107 (1989).

Appendix A

Sodium Caseinate/Xanthan Ternary Solutions

Appendix B

Guar/Dextran Ternary Solutions

Massey University
COLLEGE OF SCIENCES

Institute of
Fundamental Sciences
Physics
Private Bag 11 222
Palmerston North
New Zealand
Telephone: 64 6 356 9099
Facsimile: 64 6 350 5682
Email: ifs@massey.ac.nz
http://ifs.massey.ac.nz

15 March 2004

TO WHOM IT MAY CONCERN

MR WILLIAM NASH

Mr Nash has pursued the Doctoral course of study in accordance with the University's Doctoral regulations.

Yours sincerely

D N Pinder
Associate Professor

Massey University
COLLEGE OF SCIENCES

Institute of
Fundamental Sciences
Physics
Private Bag 11 222
Palmerston North
New Zealand
Telephone: 64 6 356 9099
Facsimile: 64 6 350 5682
Email: ifs@massey.ac.nz
http://ifs.massey.ac.nz

Work in the field of ternary polymer dynamics and dynamic light scattering has been referenced in depth.

The work has followed the appropriate research practice guidelines, the work has not been of a nature where the ethical and genetic policies have been relevant.

The thesis does not exceed 100000 words.

William Nash

D N Pinder

15/3/04

Massey University
COLLEGE OF SCIENCES

Institute of
Fundamental Sciences
Physics
Private Bag 11 222
Palmerston North
New Zealand
Telephone: 64 6 356 9099
Facsimile: 64 6 350 5682
Email: ifs@massey.ac.nz
http://ifs.massey.ac.nz

Dr. Yacine Hemar prepared the samples for investigation.

None of the material presented has been used for any other degree or diploma.

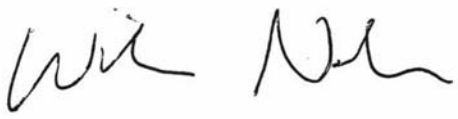

William Nash